Fourier Modal Method

Lifeng Li

Gratings:
Theory and Numeric Applications
Second Revisited Edition

Tryfon Antonakakis
Fadi Baïda
Abderrahmane Belkhir
Kirill Cherednichenko
Shane Cooper
Richard Craster
Guillaume Demesy
John DeSanto
Gérard Granet
Boris Gralak
Leonid Goray
Sébastien Guenneau
Lifeng Li
Daniel Maystre
André Nicolet
Gunther Schmidt
Brian Stout
Fréderic Zolla

Evgeny Popov, Editor

Institut Fresnel, Université d'Aix-Marseille, Marseille, France
Institut FEMTO-ST, Université de Franche-Comté, Besançon, France
Institut Pascal, Université Blaise Pascal, Clermont-Ferrand, France
Colorado School of Mines, Golden, USA
CERN, Geneva, Switzerland
Imperial College London, UK
Cardiff University, Cardiff, UK
Université Mouloud Mammeri, Tizi-Ouzou, Algeria
Saint Petersburg Academic University, Saint Petersburg, Russian Federation
Institute for Analytical Instrumentation, Saint Petersburg, Russian Federation
Weierstrass Institute of Applied Analysis and Stochastics, Berlin, Germany
Tsinghua University, Beijing, China

ISBN: 978-2-85399-943-4

www.fresnel.fr/numerical-grating-book-2

ISBN: 2-85399-943-4

Second Edition, 2014

World Wide Web:

www.fresnel.fr/numerical-grating-book-2

Aix Marseille Université, CNRS, Centrale Marseille, Institut Fresnel UMR 7249,
13397 Marseille,
France

Gratings: Theory and Numeric Applications, Second Revisited Edition, Evgeny Popov, editor (Aix Marseille Université, CNRS, Centrale Marseille, Institut Fresnel UMR 7249, 2014)

2014
Presses Universitaires de Provence

Chapter 13:

Fourier Modal Method

Lifeng Li

Table of Contents

Chapter 13

Fourier Modal Method

Lifeng Li

Department of Precision Instrument, Tsinghua University
Beijing 100084, China
lifengli@tsinghua.edu.cn

13.1 Introduction

The Fourier modal method is the most popular method for modeling diffraction gratings. The method is characterized by expanding the electromagnetic fields into Floquet-Fourier series and medium permittivity (and possibly also medium permeability) into Fourier series and solving the resulting Maxwell equations as a matrix eigenvalue problem. It is favored by researchers, engineers and graduate students who want to solve their research or engineering problems quickly. The popularity of the method is mostly due to its simplicity and partially due to its versatility. Compared with the other methods described in this book, to implement the Fourier modal method in a high-level computer language requires very few steps in programming and a minimal level of understanding of the mathematical theory behind it. The method is also fairly versatile because it can model both surface-relief gratings and volume gratings, i.e., gratings consisting of distinct periodic material boundaries and gratings having continuous periodic spatial variation of index of refraction. For a surface-relief grating of arbitrary shape, the method uses staircase approximation to approximate the profile function. When the periodic region of the grating contains only dielectric media or when the region contains metallic media but the electric field vector is everywhere parallel to the metal surfaces, the staircase approximation can produce reliable numerical results for the far field; however, when the latter condition is not met the approximation may fail to produce correct results.

There have been a couple of confusion points about the Fourier modal method. The first concerns its relationship with the so-called rigorous coupled-wave analysis. The latter name was first adopted by Moharam and Gaylord [13.1] in 1981 and it stemmed from the work of Kogelnik [13.2] in 1969 on an approximate theory for thick hologram gratings. Some people mistakenly consider that the two names refer to two related but different methods, whereas the two refer to exactly the same method since they solve the same modal equation in Fourier space. The name Fourier modal method is a better one because it reflects the essence of the method. The second confusion point is about the history of the method. Many people have been misled to believe that the method was proposed in the early 1980s [13.3, 13.4]. This is very unfortunate because the Fourier modal method has a history that is equally long as the classical differential method and integral method. For a brief review of its history the reader may consult with the introduction in [13.5].

Despite its long history and popularity, to date the Fourier modal method has not been given a complete and concise coverage in the literature. This is especially true for one-dimensional gratings in conical mounting. This chapter is an attempt to fill the void. The em-

phasis of this writing is on completeness and clarity of the formulation, and the aim is to help a reader correctly and easily implement the method in a computer code, if there is such a need.

To reach this goal within a reasonable number of pages I will cover only gratings whose surface profiles completely coincide with some Cartesian coordinate surfaces, although to achieve maximum generality without too much complication the coordinate system is assumed to be oblique. The technique of adaptive spatial resolution [13.6] and the method of matched coordinates [13.7] will not be described. To cover them it is necessary to blur the boundary between the Fourier modal method and the coordinate transformation method, but it is beyond the scope of this chapter. The Fourier factorization rules [13.5, 13.8] are assumed to be known to the reader and they will not be treated in great details. The validity and convergence rate of the Fourier modal method in the rigorous mathematical sense has rarely been addressed [13.5, 13.9] and they will not be discussed here. However, from a practical point of view the reader can be assured that the validity and accuracy of the method has been proven beyond doubt by numerous numerical tests and experimental verifications.

To make this chapter easier to read for a novice I have taken an approach of gradually increasing the difficulty of contents and brevity of description. Each section is built upon the previous one and extends the previous one in certain directions.

13.2 One-dimensional, isotropic gratings in non-conical mounting

13.2.1 General methodology

In the most general term the electromagnetic grating problem can be stated as this: given a periodic grating with known opto-geometric parameters and a monochromatic incident plane wave to find the distribution of the diffracted electromagnetic waves in the far field and near field. From an electromagnetic point of view this amounts to solving a boundary value problem. The Fourier modal method is just one way to solve this boundary value problem. The method consists of three steps. The three-dimensional physical space containing the grating is divided into three regions: the top semi-infinite transparent region where the incident plane wave comes from infinity, the middle region, also called the grating region or periodic region, where periodic variation of medium boundary or refractive indices takes place, and the bottom semi-infinite region that may be opaque. In some cases the middle region may be further divided into a few sub-regions. In the first step general expressions of the total electromagnetic fields in the individual regions (and sub-regions, if any) are found. These expressions still contain unknown coefficients. In the second step the electromagnetic boundary conditions are applied to the total fields at the interfaces between the regions and sub-regions, and the unknown coefficients are thereby determined by solving the resulting linear system of equations. In the final step the quantities of interests, e.g., diffraction efficiency, diffraction phase, state of polarization, and field distribution, etc., are extracted from the determined coefficients.

The three steps described above are actually shared by many numerical grating methods. It is the contents of the first step that distinguish one method from another. In a modal method the construction of the total electromagnetic fields is accomplished by means of modes. Mode is a powerful concept in physics. It means a distinct, self-sustainable pattern of motion that satisfies the governing law of physics including the internal boundary conditions. Just like a vibrating string has its vibrating mechanical or acoustic modes and an optical fiber has its transmission modes, a grating structure also has its electromagnetic modes. The modes of each region satisfy Maxwell equations and the associated internal boundary conditions, including the pseudo-periodicity conditions. In a modal method the solution of the total fields that satisfy the external boundary conditions between different regions and the radiation conditions at infinity is formed by superposition of all the modes, thanks to the linearity of the electromagnetic problem. In the two semi-infinite regions the total fields are given by the

Rayleigh expansions (see Chap. 2), and each term of the expansions can be rightfully viewed as a mode of the region.

The modes of the periodic region can be found in several ways. When the medium parameters and the electromagnetic fields are expanded into Fourier and Floquet-Fourier series, respectively, the resulting method of solution is called the Fourier modal method. Although in principle gratings of any groove shape possess modes, only the rectangular grating allows its modes to be easily found and lends itself as the basic object of study to the Fourier modal method. Another good reason for the Fourier modal method to be based on treatment of rectangular gratings is that a rectangle (or in general a parallelogram) is naturally a brick for building up an arbitrary grating profile (see Sect. 13.5).

In this section the Fourier modal method for the simplest grating problem, that of a rectangular grating in nonconical mounting, is formulated. Besides giving results for this simple but practically important grating case, the section also lays down the general framework for the remaining sections on more general grating shapes and plane wave incident angles.

13.2.2 Formulation in the rectangular Cartesian coordinate system

13.2.2.1 Description of the problem of rectangular gratings

Figure 13.1 depicts a rectangular grating illuminated by a monochromatic plane wave. A rectangular Cartesian coordinate system is attached to the grating with its x and y axes perpendicular and parallel to grating grooves, respectively. The xz plane is called the principal plane of the grating and the xy plane is called grating plane. The origin of the coordinate system is placed at the bottom center of one of the grooves. The grating is composed of at least two media, medium a and medium b with scalar permittivities ε_a and ε_b. The upper semi-infinite region (the cover) and the lower semi-infinite region (the substrate) are labeled with 2 and 0, and their scalar permittivities are $\varepsilon^{(2)}$ and $\varepsilon^{(0)}$. The magnetic permeabilities of all media are denoted by μ with appropriate subscripts or superscripts. Although in optical problems they are equal to that of vacuum the notation is formally retained for electromagnetic symmetry considerations. In most applications the cover is air and $\varepsilon_a = \varepsilon^{(2)}$, and very often the substrate and medium b are of the same material ($\varepsilon_b = \varepsilon^{(0)}$), so the spaces occupied by media a and b are called grooves and ridges of the grating, respectively. The grating period, groove depth, groove width, and ridge width are denoted by d, h, d_1, and w, respectively. Instead of w or d_1, the ratio w/d that is called the duty cycle (or filling factor) is often a more convenient parameter to use. For later convenience, we define two real ordinates, $z_0 = 0$ and $z_1 = h$, which are the lower and upper boundaries of the periodic layer, and two fictitious ordinates $z_{-1} = z_0$ and $z_2 = z_1$, which have no physical meanings. Note that the permittivity is a piecewise constant function of spatial variables, and in the grating region it is a periodic function of x only:

$$\varepsilon(x) = \begin{cases} \varepsilon_a, & \text{if } |x| \le d_1/2, \quad 0 \le z \le h; \\ \varepsilon_b, & \text{if } d_1/2 < |x| \le d/2, \quad 0 \le z \le h. \end{cases} \tag{13.1}$$

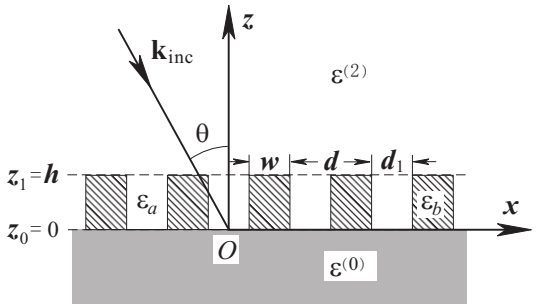

Fig. 13.1. Definition and notation of a rectangular grating problem.

The incident plane wave is characterized by its wavelength λ, wave vector $\mathbf{k}_{\text{inc}}$, and polarization vector $\hat{\mathbf{a}}$, where

$$\mathbf{k}_{\text{inc}} = k_0\sqrt{\varepsilon^{(2)}\mu^{(2)}}\,(\hat{\mathbf{x}}\sin\theta - \hat{\mathbf{z}}\cos\theta), \tag{13.2}$$

with $k_0 = 2\pi/\lambda$ being the vacuum wave vector. So, the plane of incidence coincides with the principal plane of the grating.

Since the grating structure is y invariant and the incident wave is independent of y, the electric and magnetic field vectors **E** and **H** are also independent of y. In this section we consider the TM polarization (transverse magnetic: the magnetic field vector perpendicular to the principal plane). Because we formally keep magnetic permeability μ in all formulas derived in this chapter, results for TE polarization can be easily obtained from the TM results by using the symmetry of Maxwell equations with respect to electric and magnetic quantities. The assumed harmonic time dependence in this chapter is $\exp(-i\omega t)$.

13.2.2.2 Construction of the total fields

For the TM polarization problem it is convenient to work with the y component of the magnetic vector H_y. It has been shown in Chapter 2 that the total fields in the upper and lower semi-infinite regions can be readily written as Rayleigh expansions:

$$H_y(x,z) = \exp(\mathrm{i}\alpha_0 x - \mathrm{i}\gamma_0^{(2)} z) + \sum_{m=-\infty}^{+\infty} R_m^{(\mathrm{h})} \exp(\mathrm{i}\alpha_m x + \mathrm{i}\gamma_m^{(2)} z), \qquad z \ge h; \tag{13.3a}$$

$$H_y(x,z) = \sum_{m=-\infty}^{+\infty} T_m^{(\mathrm{h})} \exp(\mathrm{i}\alpha_m x - \mathrm{i}\gamma_m^{(0)} z), \qquad z \le 0. \tag{13.3b}$$

In the above equations

$$\alpha_m = \alpha_0 + mK, \qquad \alpha_0 = k^{(2)}\sin\theta, \qquad K = 2\pi/d, \tag{13.4}$$

$$\gamma_m^{(p)} = \sqrt{k^{(p)2} - \alpha_m^2}, \qquad \mathrm{Re}[\gamma_m^{(p)}] + \mathrm{Im}[\gamma_m^{(p)}] > 0, \qquad p = 0, 2 \tag{13.5}$$

where $k^{(p)2} = k_0^2 n^{(p)2}$ with $n^{(p)} = \sqrt{\varepsilon^{(p)}\mu^{(p)}}$ being the refractive indices of the two media, and $R_m^{(\mathrm{h})}$ and $T_m^{(\mathrm{h})}$ are the unknown Rayleigh coefficients. The first term in (13.3a) represents the incident plane wave of unit amplitude. The + and – signs in front of the second terms in the exponential functions in (13.3) have been carefully chosen in accordance with the inequality in (13.5) to ensure that the radiation condition is satisfied.

Next we find the total magnetic field in the periodic layer. To do so we need first to derive the eigenvalue equation that determines the modes of the periodic layer. For time-harmonic electromagnetic fields two of the Maxwell equations containing the curl operator are

$$\nabla\times\mathbf{E} = \mathrm{i}k_0\mu\mathbf{H}, \tag{13.6a}$$

$$\nabla\times\mathbf{H} = -\mathrm{i}k_0\varepsilon\mathbf{E}. \tag{13.6b}$$

For y independent TM polarized fields these equations become

$$\partial_z E_x - \partial_x E_z = \mathrm{i}k_0\mu H_y, \tag{13.7a}$$

$$\partial_x H_y = -\mathrm{i}k_0\varepsilon E_z, \tag{13.7b}$$

$$\partial_z H_y = \mathrm{i}k_0\varepsilon E_x. \tag{13.7c}$$

Using the last two equations to eliminate E_x and E_z and keeping in mind that ε is a function of only x, one can easily find

$$k_0^2 \varepsilon \mu H_y(x,z) + \varepsilon \partial_x \frac{1}{\varepsilon} \partial_x H_y(x,z) = -\partial_z^2 H_y(x,z) \,. \tag{13.8}$$

Since the coefficients of this differential equation do not depend on z, applying the standard procedure of separation of variables shows that the equation has a solution of the form $H_y(x,z) = H_y(x)\exp(i\gamma z)$, where γ is a constant. Substituting this into (13.8) yields

$$k_0^2 \varepsilon \mu H_y + \varepsilon \frac{\mathrm{d}}{\mathrm{d}x} \frac{1}{\varepsilon} \frac{\mathrm{d}}{\mathrm{d}x} H_y = \gamma^2 H_y \,. \tag{13.9}$$

Henceforth H_y without an explicit variable dependence denotes the function $H_y(x)$. The ordinary differential equation (13.9) together with the associated boundary conditions defines an eigenvalue problem with γ being the eigenvalue. Here the boundary conditions are of two kinds. The first kind is the electromagnetic boundary conditions at the permittivity jump discontinuities. Obviously, being a tangential component to the medium interface H_y is continuous, and it follows from (13.7b) $(1/\varepsilon)\partial_x H_y$ must also be continuous:

$$H_y(\pm d_1/2 \pm 0) = H_y(\pm d_1/2 \mp 0), \quad \frac{1}{\varepsilon_b} \frac{\mathrm{d}H_y}{\mathrm{d}x}(\pm d_1/2 \pm 0) = \frac{1}{\varepsilon_a} \frac{\mathrm{d}H_y}{\mathrm{d}x}(\pm d_1/2 \mp 0) \,. \tag{13.10}$$

By the way, if (13.9) is understood in the sense of distribution, (13.10) is already contained in it. The second kind of boundary condition to be imposed on (13.9) is the pseudo-periodicity condition. Since $\varepsilon(x+d) = \varepsilon(x)$ appears in the coefficients of (13.9), Floquet theorem requires that $H_y(x)$ be pseudo-periodic

$$H_y(x+d) = \exp(\mathrm{i}\alpha_0 d) H_y(x) \,, \tag{13.11}$$

where α_0 is the pseudo-periodicity constant determined by the incident plane wave.

A solution of the eigenvalue problem defined by (13.9-11) is an eigenvalue and eigenfunction pair $\{\gamma, H_y(x;\gamma)\}$. An eigen-function $H_y(x;\gamma)$ is in physical term a mode of the lamellar grating structure. For mode $H_y(x;\gamma)$ the law of motion is (13.9) and the internal boundary conditions are (13.10) and (13.11). Effectively the problem is that of finding modes of a periodic waveguide. Because $H_y(x,z) = H_y(x;\gamma)\exp(i\gamma z)$ the x dependence of the modal field is independent of z. In searching for the eigen-solutions the z invariance of ε is used, as if the grating layer is infinitely thick. The finiteness of the grating layer is not recalled until the external boundary conditions are matched between different regions in the next step.

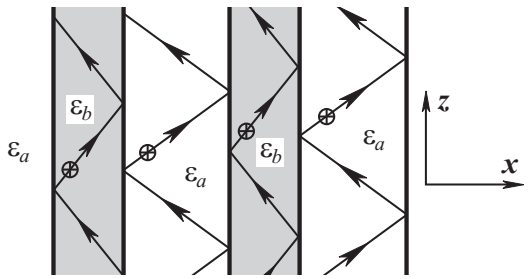

Fig. 13.2. Geometric optics picture of a mode of a periodic waveguide. The arrows represent optical rays and $\oplus$ represent the direction of the electric vector in TE polarization or that of the magnetic vector in TM polarization.

For a piecewise homogeneous periodic region the modal function has a simple geometric optics interpretation. In each medium the function is composed of two plane waves whose wave vectors share the same z component γ and have x components of equal length but opposite signs, as shown in Fig. 13.2. The zigzag paths can be understood as optical rays. In differ-

ent media the zigzag paths make different angles with respect to the x axis, but the z components of their associated wave vectors are the same. Since different modes have different eigenvalues γ the angles of zigzag paths for different modes within a given medium are also different. The phases of the ray paths at the same ordinate z and two abscissas differing by d are related by Floquet theorem. The planes of all zigzag paths are perpendicular to the medium interfaces. The periodic region allows two characteristic polarizations, one with its magnetic field vector perpendicular to the zigzag plane, which is the present case, and the other with its electric field vector perpendicular to the zigzag plane, which corresponds to TE polarization incidence. The zigzag path angles for TE polarization are in general different from those for TM polarization.

The eigenvalue spectrum of (13.9) is composed of a discrete set of numbers. Since γ appears in (13.9) as γ^2, if γ is an eigenvalue, so is $-\gamma$, and $\pm\gamma$ share the same eigen-function $H_y(x)$. In actual manipulation γ is chosen as one of the two square roots of γ^2. We only need to label half of the eigenvalues using index q = 1, 2, …; the second half is referenced by adding a negative sign in front of the first half. When we limit our domain of discussion within the linear electromagnetic problems a linear superposition of modal fields is also a solution of Maxwell equations. A general solution in the grating layer satisfying all internal boundary conditions is given by a superposition of all possible modes

$$H_y(x,z) = \sum_{q=1}^{\infty} [\, u_q \exp(\mathrm{i}\gamma_q z) + d_q \exp(-\mathrm{i}\gamma_q z)\,] H_{y,q}(x), \tag{13.12}$$

where u_q and d_q are constants, and a comma is used in the subscript for $H_{y,q}(x)$ for a reason to become clear soon. When $H_{y,q}(x)$ are properly normalized, u_q and d_q are the modal amplitudes evaluated at z = 0. Since (13.12) is valid for z being finite, no radiation condition is to be imposed and both terms with the + and – signs in the exponential functions should be kept. In this sense it is not important how γ_q is chosen from the two square roots. However, to attach an unambiguous physical meaning to each term and to facilitate later numerical treatment, eigenvalue partition must be made. As with the $\gamma_m^{(l)}$ appearing in Rayleigh expansions, we require

$$\gamma_q = \sqrt{\gamma_q^2}\,, \qquad \mathrm{Re}[\gamma_q] + \mathrm{Im}[\gamma_q] > 0. \tag{13.13}$$

Then, the first term in (13.12) represents a mode that propagates or decays in the upward direction, and the second term represents a mode in the downward direction, justifying the choice of letters for the two superposition constants.

So far we have not discussed how to obtain the eigen-functions $H_{y,q}(x)$. In the Fourier modal method they are obtained by solving (13.9) in the discrete Fourier space. For this purpose $H_y(x)$ is expanded into Floquet-Fourier series

$$H_y(x) = \sum_{m=-\infty}^{\infty} H_{ym} \exp(\mathrm{i}\alpha_m x), \tag{13.14}$$

where α_m is defined in (13.4) and H_{ym} are the Fourier coefficients (for convenience we will indistinguishably refer to both Fourier and Floquet-Fourier coefficients as Fourier coefficients). Note that to distinguish from the qth eigen-function $H_{y,q}(x)$, the subscript in H_{ym} does not contain a comma. In this chapter when a roman letter subscript in italics such as m and n is attached to a symbol representing a function of spatial variables, the composite symbol denotes the Fourier coefficients of the function.

Equation (13.9) also contains $\varepsilon(x)$ that too has to be transformed into Fourier space. It is tempting to expand $\varepsilon(x)$ into a Fourier series and substitute it, together with (13.14), into (13.9) to derive the desired result. This is how it was done before 1996; however, numerically the resulting solution converged very slowly when medium a or b was a highly conducting metal.

It was later found that only when the Fourier coefficients were used in a special way the Fourier modal method could converge well for metallic rectangular gratings [13.10, 13.11]. This finding led to establishment of a theory called Fourier factorization [13.8], which not only explained the observed improvement of convergence in [13.10, 13.11] but also enabled a series of other improvements in grating theory. However, it would take us afield to cover this topic at length in this chapter, so I am content with giving only key results here. The interested reader can find more information in [13.5, 13.8], and Chapter 7 of this book.

Given a function $h(x)$ as the product of two periodic, piecewise continuous functions $g(x)$ and $f(x)$, all three functions having the same period, to compute the Fourier coefficients of $h(x)$ in terms of the Fourier coefficients of $g(x)$ and $f(x)$ one should follow the Fourier factorization rules:

(1) If $g(x)$ is discontinuous and $f(x)$ is continuous, then

$$h_{n,\Omega} = \sum_{m\in\Omega} g_{n-m} f_m, \qquad n \in \Omega. \tag{13.15}$$

(2) If both $g(x)$ and $f(x)$ are discontinuous but $g(x)f(x)$ is continuous, then

$$h_{n,\Omega} = \sum_{m\in\Omega} \left[\!\!\left[\frac{1}{g} \right]\!\!\right]^{-1}_{\Omega,nm} f_m, \qquad n \in \Omega. \tag{13.16}$$

(3) If $g(x)$ and $f(x)$ meet neither of the above two conditions, do not use (13.15) or (13.16) directly. Instead, rearrange $g(x)f(x)$ as a sum of several terms so that each term meets one of the two conditions, and then follow (1) and (2).

In the above Ω denotes a set of integers: $m_1 \le m \le m_2$ for some fixed m_1 and m_2. $[\![a]\!]$ Denotes the square Toeplitz matrix generated by the Fourier coefficients of function $a(x)$ such that $[\![a]\!]_{mn} = a_{m-n}$, and $[\![a]\!]^{-1}$ means the matrix inverse of $[\![a]\!]$. The subscript Ω on the right-hand side of (13.16) is used to indicate the size of the matrix and that on the left-hand side of both equations are to indicate that these Fourier coefficients depend on Ω. When there is no danger of confusion, Ω can be omitted.

The three types of products in (1), (2), and (3) are referred to as Type 1, Type 2, and Type 3 products, respectively. From a mathematical point of view (13.15) and (13.16) give two multiplication rules for multiplying two Fourier series in a truncated Fourier space delimited by Ω. The one in (13.15) is called Laurent's rule and that in (13.16) is called the inverse rule. Although the factorization rules are stated for $h(x)$, $f(x)$, and $g(x)$ all being periodic functions, they are obviously valid when $h(x)$ and $f(x)$ are pseudo-periodic because we can multiply $h(x) = g(x)\,f(x)$ by $\exp(-i\alpha_0 x)$.

The essence of following the Fourier factorization rules is to preserve continuity nature of the product function. While the pseudo-periodicity condition is automatically satisfied once $H_{ay}(x)$ is expanded into Floquet-Fourier series as in (13.14), the internal electromagnetic boundary conditions (13.10) have to be expressly enforced. Equation (13.9) contains three products of periodic and pseudo-periodic functions: εH_y, $(1/\varepsilon)H_y'$, and $\varepsilon\,[(1/\varepsilon)H_y']'$, where the prime denotes derivative with respect to x. They are of Types 1, 2, and 3, respectively. The presence of the Type 3 product prevents a direct Fourier factorization of (13.9). The difficulty can be avoided by rewriting (13.9) as

$$\varepsilon\left(k_0^2 \mu H_y + \frac{\mathrm{d}}{\mathrm{d}x}\frac{1}{\varepsilon}\frac{\mathrm{d}}{\mathrm{d}x} H_y \right) = \gamma^2 H_y\,. \tag{13.17}$$

This new equation contains only Type 2 products. Before making the Fourier transform let us note that the action of the differential operator d/dx on a pseudo-periodic series is to multiply its nth term by $i\alpha_n$ for all n. Then the image of (13.9) in discrete Fourier space is

$$\left[\!\left[\frac{1}{\varepsilon}\right]\!\right]^{-1}\left(k_0^2\mu\mathbf{I}-\boldsymbol{\alpha}\left[\!\left[\varepsilon\right]\!\right]^{-1}\boldsymbol{\alpha}\right)H_y=\gamma^2 H_y\,, \tag{13.18}$$

where $\mathbf{I}$ is the identity matrix, $\boldsymbol{\alpha}$ is a diagonal matrix with α_n being its diagonal elements, and without possibility of confusion we have used H_y to denote the column vector formed by H_{ym}, the Fourier coefficients of $H_y(x)$. Note that equation (13.18) contains all three ingredients of our boundary value problem in one equation.

Equation (13.18) can also be derived by first transforming (13.7) into Fourier space and then eliminating the column vectors formed by the Fourier coefficients of $E_x(x)$ and $E_z(x)$. We will see in later sections, it is always easier to transform the original Maxwell equations into Fourier space when products of functions are simple and then to carry out the necessary manipulations in Fourier space, than to defer the transformation until a later or the final stage when the products of functions involved in a wave equation have become more complicated.

Equation (13.18) is written in the standard form of a matrix eigenvalue problem. It can be solved numerically by using an eigenvalue-eigenvector solver available in many computer software packages. When the matrix in (13.18) is truncated to $N \times N$, where $N = m_2 - m_1 + 1$ is the number of elements in set Ω, the number of eigen-solutions is N, but after taking square roots of γ^2 there are $2N$ eigen-solutions to the underlying physical problem. Criterion (13.13) may be used to make the eigenvalue spectrum partition. In comparison with (13.12) the total magnetic field is now written as a Floquet-Fourier series

$$H_y(x,z)=\sum_{m=m_1}^{m_2}\exp(\mathrm{i}\alpha_m x)\sum_{q=1}^{N}H_{ymq}\left[u_q\exp(\mathrm{i}\gamma_q z)+d_q\exp(-\mathrm{i}\gamma_q z)\right], \tag{13.19}$$

where H_{ymq} are the Fourier coefficients of $H_{y,q}(x)$. So far we have derived the general expressions of the total magnetic field in all three spatial regions. These expressions contain the unknown modal amplitudes u_q and d_q and the unknown Rayleigh coefficients (that can be considered as special modal amplitudes).

Before moving on to solve for the unknown coefficients we comment on the practical issue of truncation. The truncation number N determines the accuracy of the numerical results; the larger N is the more accurate the results are but the more computation time and computer memory are consumed. N should be chosen large enough to include all propagating orders and sufficiently many evanescent orders on both side of the propagating orders. How large is sufficient depends on the specific problem. It is difficult to give a general criterion. Certainly a metallic grating requires a larger N than does a dielectric grating, and a grating of near zero or near 100% duty cycle requires a larger N than does a grating of 50% duty cycle. The best way to be sure is to run a few convergence tests. The minimum N beyond which the numerical results of quantities of interest stabilize is a good truncation number to use. It is a common practice that the truncation interval $[m_1,m_2]$ is chosen as $[-M,M]$ for some $M > 0$; however, it is better to set $m_1 = -[\alpha_0/K] - [N/2]$, where $[\cdot]$ means the integral part of. In this way good truncation coverage is achieved even when the angle of incidence is near grazing.

13.2.2.3 Matching of the external boundary conditions

In the Fourier modal method the matching of boundary conditions between different regions is realized by matching the Fourier coefficients of the tangential components of the total fields. In the preceding subsection the total magnetic fields in the three regions have been written in Floquet-Fourier series. The other tangential component, the x component of the electric field,

is yet to be found and written in this form. Equation (13.7c) provides the link between E_x and H_y:

$$E_x = \frac{1}{\mathrm{i}k_0\varepsilon}\partial_z H_y \,. \tag{13.20}$$

In regions 0 and 2, ε is a constant, so it follows easily from (13.3) that

$$E_x(x,z) = \frac{1}{k_0\varepsilon^{(2)}}\left[-\gamma_0^{(2)}\exp(\mathrm{i}\alpha_0 x - \mathrm{i}\gamma_0^{(2)} z) + \sum_{m=-\infty}^{+\infty}\gamma_m^{(2)} R_m^{(\mathrm{h})}\exp(\mathrm{i}\alpha_m x + \mathrm{i}\gamma_m^{(2)} z)\right], \quad z \geq h; \tag{13.21a}$$

$$E_x(x,z) = -\frac{1}{k_0\varepsilon^{(0)}}\sum_{m=-\infty}^{+\infty}\gamma_m^{(0)} T_m^{(\mathrm{h})}\exp(\mathrm{i}\alpha_m x - \mathrm{i}\gamma_m^{(0)} z), \quad z \leq 0. \tag{13.21b}$$

In the periodic layer, the Floquet-Fourier series of E_x in terms of H_y is obtained by transforming the right-hand side of (13.20) into Fourier space using Laurent's rule:

$$E_x(x,z) = \frac{1}{k_0}\sum_{m=m_1}^{m_2}\exp(\mathrm{i}\alpha_m x)\sum_{n=m_1}^{m_2}\left[\!\left[\frac{1}{\varepsilon}\right]\!\right]_{mn}\sum_{q=1}^{N}\gamma_q H_{ynq}\left[u_q\exp(\mathrm{i}\gamma_q z) - d_q\exp(-\mathrm{i}\gamma_q z)\right]. \tag{13.22}$$

Equations (13.3), (13.19), (13.21), and (13.22) provide the Fourier coefficients of all vector field components needed to match boundary conditions.

To facilitate subsequent development it is convenient to define two column vectors. The first is the vector of modal amplitudes:

$$F = \begin{pmatrix}\tilde{u}_q \\ \tilde{d}_q\end{pmatrix}, \tag{13.23}$$

where $\tilde{u}_q$ and $\tilde{d}_q$ are the qth upward and downward modal amplitudes evaluated at the lower and upper boundaries of the grating layer, respectively:

$$\tilde{u}_q = u_q\exp(\mathrm{i}\gamma_q z_0), \qquad \tilde{d}_q = d_q\exp(-\mathrm{i}\gamma_q z_1). \tag{13.24}$$

In (13.23) a generic vector element is used to represent the whole sub-vector. So, if the number of modes to be used in numerical computation is N, then $\tilde{u}_q$ and $\tilde{d}_q$ each represents an $N \times 1$ column vector with $1 \leq q \leq N$. (13.23) is written for the periodic layer. In the upper semi-infinite space $\tilde{u}_q$ and $\tilde{d}_q$ are to be replaced by $\tilde{R}_m^{(\mathrm{h})}$ and $\tilde{\delta}_{mn}$, and in the lower semi-infinite space by 0 and $\tilde{T}_m^{(\mathrm{h})}$, respectively, where

$$\tilde{R}_m^{(\mathrm{h})} = R_m^{(\mathrm{h})}\exp(\mathrm{i}\gamma_m^{(2)} z_1), \quad \tilde{T}_m^{(\mathrm{h})} = T_m^{(\mathrm{h})}\exp(-\mathrm{i}\gamma_m^{(0)} z_0), \quad \tilde{\delta}_{mn} = \delta_{mn}\exp(-\mathrm{i}\gamma_m^{(2)} z_2), \tag{13.25}$$

and $\delta_{mn} = 0$ for $m \neq n$ and $\delta_{mn} = 1$ for $m = n$. The second vector to define is the vector of Fourier coefficients of the total fields

$$\mathscr{F}(z) = \begin{pmatrix}H_{ym}(z) \\ E_{xm}(z)\end{pmatrix}, \tag{13.26}$$

where H_{ym} and E_{xm} are also short-hand notations of $N \times 1$ column vectors. In terms of these column vectors the Fourier coefficients of the total fields in the three spatial regions are

$$\mathscr{F}(z) = \mathbf{W}^{(2)}\phi^{(2)}(z)\begin{pmatrix}\tilde{R}_m^{(\mathrm{h})}\\ \tilde{\delta}_{m0}\end{pmatrix}, \qquad z \ge z_1; \tag{13.27a}$$

$$\mathscr{F}(z) = \mathbf{W}^{(1)}\,\phi^{(1)}(z)\begin{pmatrix}\tilde{u}_q\\ \tilde{d}_q\end{pmatrix}, \qquad z_0 \le z \le z_1; \tag{13.27b}$$

$$\mathscr{F}(z) = \mathbf{W}^{(0)}\phi^{(0)}(z)\begin{pmatrix}0\\ \tilde{T}_m^{(\mathrm{h})}\end{pmatrix}, \qquad z \le z_0, \tag{13.27c}$$

where

$$\phi^{(p)}(z) = \begin{pmatrix}\exp[\mathrm{i}\,\gamma_m^{(p)}(z - z_{p-1})] & 0\\ 0 & \exp[\mathrm{i}\,\gamma_m^{(p)}(z_p - z)]\end{pmatrix}, \qquad p = 0, 2, \tag{13.28a}$$

$$\phi^{(1)}(z) = \begin{pmatrix}\exp[\mathrm{i}\,\gamma_q\,(z - z_0)] & 0\\ 0 & \exp[\mathrm{i}\,\gamma_q\,(z_1 - z)]\end{pmatrix}, \tag{13.28b}$$

$$\mathbf{W}^{(p)} = \begin{pmatrix}\delta_{mn} & \delta_{mn}\\ \dfrac{\gamma_m^{(p)}}{k_0\varepsilon^{(p)}}\delta_{mn} & -\dfrac{\gamma_m^{(p)}}{k_0\varepsilon^{(p)}}\delta_{mn}\end{pmatrix}, \qquad p = 0, 2, \tag{13.29a}$$

$$\mathbf{W}^{(1)} = \begin{pmatrix}H_{ymq} & H_{ymq}\\ \dfrac{1}{k_0}\displaystyle\sum_{n=m_1}^{m_2}\left[\!\left[\frac{1}{\varepsilon}\right]\!\right]_{mn} H_{ynq}\gamma_q & -\dfrac{1}{k_0}\displaystyle\sum_{n=m_1}^{m_2}\left[\!\left[\frac{1}{\varepsilon}\right]\!\right]_{mn} H_{ynq}\gamma_q\end{pmatrix}. \tag{13.29b}$$

In all of the above matrices a generic matrix element represents a matrix. For example, H_{ymq} stands for the square matrix and $\exp(i\gamma_q z)$ stands for the diagonal matrix. All matrices in (13.27-29) are of finite size, truncated from $m = m_1$ to $m_2 = N + m_1 - 1$, or from $q = 1$ to N. Note that all $\mathbf{W}$ matrices have a symmetric structure: If W_{ij}, where $i, j = 1, 2$, are used to denote the 2×2 block matrices, then $W_{12} = W_{11}$ and $W_{22} = -W_{21}$. This symmetry property can be exploited to save computation time [13.12]. With all of the above notations the matching of the boundary conditions at $z = z_0$ and $z = z_1$ can be written as $\mathscr{F}(z_1 + 0) = \mathscr{F}(z_1 - 0)$:

$$\mathbf{W}^{(2)}\phi^{(2)}(z_1)\begin{pmatrix}\tilde{R}_m^{(\mathrm{h})}\\ \tilde{\delta}_{m0}\end{pmatrix} = \mathbf{W}^{(1)}\,\phi^{(1)}(z_1)\begin{pmatrix}\tilde{u}_q\\ \tilde{d}_q\end{pmatrix}, \tag{13.30a}$$

and $\mathscr{F}(z_0 + 0) = \mathscr{F}(z_0 - 0)$:

$$\mathbf{W}^{(1)}\,\phi^{(1)}(z_0)\begin{pmatrix}\tilde{u}_q\\ \tilde{d}_q\end{pmatrix} = \mathbf{W}^{(0)}\phi^{(0)}(z_0)\begin{pmatrix}0\\ \tilde{T}_m^{(\mathrm{h})}\end{pmatrix}. \tag{13.30b}$$

13.2.2.4 Solution of the boundary matching equations

Equations (13.30a) and (13.30b) has this general form

$$\mathbf{W}^{(p+1)}\begin{pmatrix}1 & 0\\ 0 & \exp(\mathrm{i}\gamma_q^{(p+1)}h_{p+1})\end{pmatrix}\begin{pmatrix}\tilde{u}_q^{(p+1)}\\ \tilde{d}_q^{(p+1)}\end{pmatrix}=\mathbf{W}^{(p)}\begin{pmatrix}\exp(\mathrm{i}\gamma_q^{(p)}h_p) & 0\\ 0 & 1\end{pmatrix}\begin{pmatrix}\tilde{u}_q^{(p)}\\ \tilde{d}_q^{(p)}\end{pmatrix}, \tag{13.31}$$

with

$$\tilde{u}_q^{(p)}=u_q^{(p)}\exp(\mathrm{i}\gamma_q^{(p)}z_{p-1}),\qquad \tilde{d}_q^{(p)}=d_q^{(p)}\exp(-\mathrm{i}\gamma_q^{(p)}z_p), \tag{13.32}$$

provided that $h_p = z_p - z_{p-1}$ and $(\tilde{u}_q^{(p)}, \tilde{d}_q^{(p)})^{\mathrm{T}}$ is understood as the column vector composed of the Rayleigh amplitudes when p refers to a semi-infinite medium. This type of boundary matching equation is not unique in the Fourier modal method. It is shared by many other grating methods although the compositions of their **W** matrices are different. When the boundary matching equations have been derived the grating problem is nearly solved. The remaining steps, which are more or less the same for all grating methods, are to solve the resulting linear system of equations for the unknown Rayleigh amplitudes $\tilde{R}_m^{(\mathrm{h})}$ and $\tilde{T}_m^{(\mathrm{h})}$, and possibly also the internal modal amplitudes $\tilde{u}_q$ and $\tilde{d}_q$. From these amplitudes the diffraction efficiencies and parameters of polarization states can be easily obtained.

In principle many algorithms can be used to solve the boundary matching equations. Because of the appearance of the exponential functions in (13.31), some of the solution methods are numerically stable and some are not. Among the numerically stable algorithms the best method is the S matrix propagation algorithm [13.12-14]. It has the advantages of having the most clear physical meaning and the best computation efficiency. Many variants of the S matrix algorithm exist; one of them is described in Section 13.5 for the general multilayered grating problem.

13.2.2.5 Final solution of the grating problem

The diffraction efficiency of a propagating order is defined as the ratio of the z component of the Poynting vector of that order to the z component of the Poynting vector of the incident plane wave. After $R_m^{(\mathrm{h})}$ and $T_m^{(\mathrm{h})}$ have been obtained the TM diffraction efficiencies can be easily found (cf. Chap. 2):

$$\eta_{m,\mathrm{TM}}^{(2)}=\frac{\gamma_m^{(2)}}{\gamma_0^{(2)}}|R_m^{(\mathrm{h})}|^2,\qquad m\in U^{(2)}, \tag{13.33a}$$

$$\eta_{m,\mathrm{TM}}^{(0)}=\frac{\varepsilon^{(2)}\gamma_m^{(0)}}{\varepsilon^{(0)}\gamma_0^{(2)}}|T_m^{(\mathrm{h})}|^2,\qquad m\in U^{(0)}, \tag{13.33b}$$

where $\eta_{m,\mathrm{TM}}^{(2)}$ and $\eta_{m,\mathrm{TM}}^{(0)}$ are the mth-order diffraction efficiencies in the reflection and transmission sides of the grating, respectively, and $U^{(p)}$ is the set of propagating order numbers in medium p, $p = 0, 2$.

In this section we have dealt with only the TM polarization. The results for TE polarization can be easily obtained by formally making exchanges $\mathbf{E} \leftrightarrow \mathbf{H}$ and $\varepsilon \leftrightarrow -\mu$ and changing the superscripts of the Rayleigh amplitudes from (h) to (e) in all formulas derived in this section. In particular, the TE diffraction efficiencies are

$$\eta_{m,\mathrm{TE}}^{(2)}=\frac{\gamma_m^{(2)}}{\gamma_0^{(2)}}|R_m^{(\mathrm{e})}|^2,\qquad m\in U^{(2)}, \tag{13.34a}$$

$$\eta_{m,\mathrm{TE}}^{(0)}=\frac{\mu^{(2)}\gamma_m^{(0)}}{\mu^{(0)}\gamma_0^{(2)}}|T_m^{(\mathrm{e})}|^2,\qquad m\in U^{(0)}. \tag{13.34b}$$

Note that because the definitions of $\gamma_m^{(p)}$ are independent of polarization, the diffraction angles and the number of propagating orders are also independent of polarization.

13.2.3 Formulation in an oblique Cartesian coordinate system

13.2.3.1 Description of the problem of slanted gratings

The rectangular grating shown in Fig. 13.1 has the mirror reflection symmetry with respect to the *yz* plane. In many applications it is desirable to break this symmetry. A surface relief grating with its two sidewalls of a ridge parallel to each other but tilted with respect to the *yz* plane is called a slanted grating. As a typical example a parallelogram grating is shown in Fig. 13.3. All previously defined symbols have the same meanings as in Fig. 13.1. The angle ζ is called the slant angle of the grating (in the figure $\zeta > 0$). *D* is the period of the slanted slabs or fringes. The groove depth measured along the slant direction is $\tilde{h} = h/\cos\zeta$. For this type of gratings it is obvious that the rectangular staircase approximation as illustrated in the left part of the figure is very inefficient.

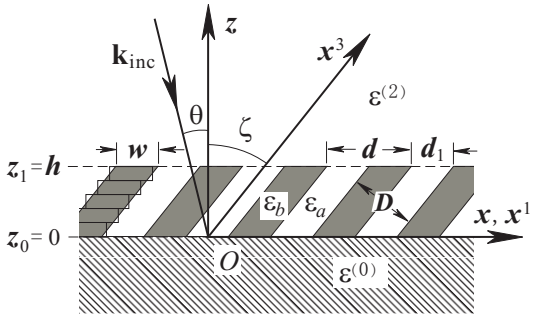

Fig. 13.3. Definition and notation of a slanted grating problem.

So far the theoretical treatments of slanted gratings have been made almost exclusively in rectangular Cartesian coordinate systems. Some authors use only one rectangular system like the one in Fig. 13.3, and others use a second rectangular system that is aligned with the surface and the normal of groove sidewalls. In either case the resulting mathematical treatments are difficult, if not awkward. However, there is nothing sacred about the rectangular coordinate system. For a parallelogram grating it is the most natural to use the oblique Cartesian coordinate system as shown in Fig. 13.3, in which every piece of flat surfaces of the grating coincides with a coordinate surface. It will be demonstrated that the Fourier modal method can be formulated the most efficiently in the matched oblique coordinate system. A small price to pay is to be familiar with properties of the uncommon oblique coordinate system.

13.2.3.2 Oblique Cartesian coordinate system

In Fig. 13.3 the rectangular coordinate system *Oxyz* is set up in the same way as in Fig. 13.1, with the *y* axis parallel to the groove direction and the *z* axis perpendicular to the grating plane. The oblique coordinate system $Ox^1x^2x^3$ is set up such that the x^1 and x^2 axes are parallel to the *x* and *y* axes, respectively, and the x^3 axis is in the *xz* plane and forms an angle ζ with respect to the *z* axis. The coordinate transformation from *Oxyz* to $Ox^1x^2x^3$ is

$$x^1 = x - z\tan\zeta, \qquad x^2 = y, \qquad x^3 = z/\cos\zeta, \tag{13.35a}$$

and the inverse transformation is

$$x = x^1 + x^3\sin\zeta, \qquad y = x^2, \qquad z = x^3\cos\zeta. \tag{13.35b}$$

For the oblique coordinate system we define three basis vectors $\mathbf{b}_1$, $\mathbf{b}_2$, and $\mathbf{b}_3$ of unit length that are in the positive directions of the x^1, x^2, and x^3 axes, respectively. From Fig. 13.3 it follows that in terms of basis vectors of *Oxyz*,

$$\mathbf{b}_1 = \hat{\mathbf{x}}, \qquad \mathbf{b}_2 = \hat{\mathbf{y}}, \qquad \mathbf{b}_3 = \hat{\mathbf{x}} \sin\zeta + \hat{\mathbf{z}} \cos\zeta . \tag{13.36}$$

We define another set of basis vectors, not necessarily of unit length by

$$\mathbf{b}^1 = \frac{\mathbf{b}_2 \times \mathbf{b}_3}{\sqrt{g}}, \qquad \mathbf{b}^2 = \frac{\mathbf{b}_3 \times \mathbf{b}_1}{\sqrt{g}}, \qquad \mathbf{b}^3 = \frac{\mathbf{b}_1 \times \mathbf{b}_2}{\sqrt{g}}, \tag{13.37}$$

where $\sqrt{g} = \mathbf{b}_1 \cdot \mathbf{b}_2 \times \mathbf{b}_3 = \cos\zeta$. From (13.36) it follows that

$$\mathbf{b}^1 = \hat{\mathbf{x}} - \hat{\mathbf{z}} \tan\zeta , \qquad \mathbf{b}^2 = \hat{\mathbf{y}}, \qquad \mathbf{b}^3 = \hat{\mathbf{z}} / \cos\zeta . \tag{13.38}$$

The basis vectors $\mathbf{b}^1$, $\mathbf{b}^2$, and $\mathbf{b}^3$ are called reciprocal space basis vectors or contravariant basis vectors, and $\mathbf{b}_1$, $\mathbf{b}_2$, and $\mathbf{b}_3$ are called the real space basis vectors or covariant basis vectors. The two sets are mutually orthonormal: $\mathbf{b}_\sigma \cdot \mathbf{b}^\rho = \delta_\sigma^\rho$, where $\delta_\sigma^\rho = 1$ if $\sigma = \rho$ and $\delta_\sigma^\rho = 0$ if $\sigma \neq \rho$. Figure 13.4 illustrates the relationship between $\mathbf{b}_\sigma$ and $\mathbf{b}^\rho$ in the x^1x^3 plane. We define covariant and contravariant metric tensors as

$$g_{\rho\sigma} = \mathbf{b}_\rho \cdot \mathbf{b}_\sigma , \qquad g^{\rho\sigma} = \mathbf{b}^\rho \cdot \mathbf{b}^\sigma , \tag{13.39}$$

respectively. In this chapter we use lowercase Greek letters ρ, σ, and τ to label components of vectors and tensors, lowercase roman letters *i*, *j*, *m*, and *n* to label Fourier coefficients of field components and permittivity and permeability tensors, and letter *q* to label eigensolutions.

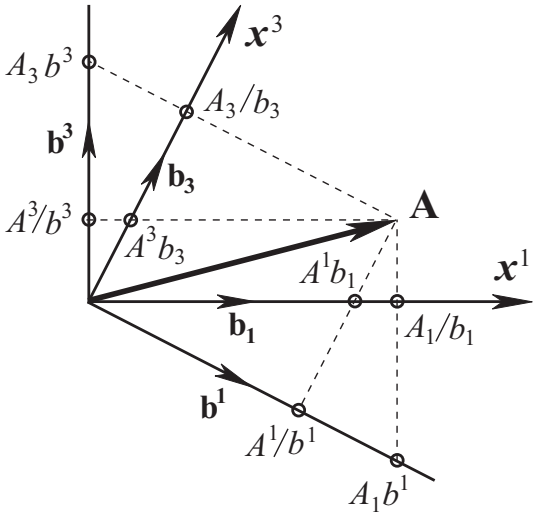

Fig. 13.4. Relationships between basis vectors and geometric interpretations of covariant and contravariant components of a vector.

An arbitrary vector can be expressed using covariant or contravariant basis vectors:

$$\mathbf{A} = A_\sigma \mathbf{b}^\sigma = A^\sigma \mathbf{b}_\sigma , \tag{13.40}$$

where summation from 1 to 3 with respect to a pair of subscript and superscript of the same symbol is implied and A_σ and A^σ are called the covariant and contravariant components of vector $\mathbf{A}$, respectively. The metric tensors provide the links between A_σ and A^σ:

$$A_\rho = g_{\rho\sigma} A^\sigma , \qquad A^\rho = g^{\rho\sigma} A_\sigma . \tag{13.41}$$

The geometrical meanings of these vector components can be summarized as follows. A_ρ is the perpendicular projection of **A** on the $\mathbf{b}_\rho$ direction in unit of $1/b_\rho$ and the parallel projection of **A** on the $\mathbf{b}^\rho$ direction in unit of b^ρ; A^ρ is the parallel projection of **A** on the $\mathbf{b}_\rho$ direction in unit of b_ρ and the perpendicular projection of **A** on the $\mathbf{b}^\rho$ direction in unit of $1/b^\rho$. The physical significance of these geometrical properties lies in the fact that many physical laws are expressed in terms of vector components in the sense of perpendicular projections. For example, the electromagnetic boundary conditions are the continuities of the tangential components of the electric and magnetic field vectors and the normal components of the electric displacement and magnetic inductance vectors across a medium interface. Here tangential and normal components are understood as the perpendicular projections of the vectors. In solving an electromagnetic boundary value problem whenever possible it is best to set up the coordinate system so that the medium interfaces are coordinate surfaces. Then the covariant and the contravariant components are proportional to the tangential and normal components, respectively, to the medium interfaces.

13.2.3.3 Construction of the total fields

To facilitate the matching of boundary conditions in the present case the Rayleigh expansions should be written in the oblique coordinates. By following steps similar to those taken in Chap. 2 for deriving Rayleigh expansions in the rectangular coordinate system, one can find

$$H_2(x^1,x^3)=\exp(\mathrm{i}\alpha_0 x^1+\mathrm{i}\gamma_0^{(2)-}x^3)+\sum_{m=-\infty}^{+\infty}R_m^{(\mathrm{h})}\exp(\mathrm{i}\alpha_m x^1+\mathrm{i}\gamma_m^{(2)+}x^3),\quad x^3\ge\tilde{h};\tag{13.42a}$$

$$H_2(x^1,x^3)=\sum_{m=-\infty}^{+\infty}T_m^{(\mathrm{h})}\exp(\mathrm{i}\alpha_m x^1+\mathrm{i}\gamma_m^{(0)-}x^3),\qquad x^3\le 0,\tag{13.42b}$$

where

$$\begin{aligned}&\gamma_m^{(p)\pm}=\alpha_m\sin\zeta\pm\sqrt{k^{(p)2}-\alpha_m^2}\,\cos\zeta,\\ &\mathrm{Re}[\sqrt{k^{(p)2}-\alpha_m^2}\,]+\mathrm{Im}[\sqrt{k^{(p)2}-\alpha_m^2}\,]>0,\end{aligned}\qquad p=0,2,\tag{13.43}$$

and α_m are still given by (13.4). Evidently here $\gamma_m^{(p)\pm}$ play the roles that $\pm\gamma_m^{(p)}$ play in (13.3). The square root selection criterion in (13.43) ensures that the terms in (13.42) have proper physical meanings.

To find the modal fields in the periodic layer we use the two curl equations of Maxwell written in the oblique Cartesian coordinate form:

$$\xi^{\rho\sigma\tau}\partial_\sigma E_\tau=\mathrm{i}k_0\mu\sqrt{g}\,H^\rho,\tag{13.44a}$$

$$\xi^{\rho\sigma\tau}\partial_\sigma H_\tau=-\mathrm{i}k_0\varepsilon\sqrt{g}\,E^\rho,\tag{13.44b}$$

where $\xi^{\rho\sigma\tau}=+1$ or -1 when $\{\rho,\sigma,\tau\}$ is an even or odd permutation of $\{1,2,3\}$, respectively, and $\xi^{\rho\sigma\tau}=0$ if any two of the indices are the same. Equation (44) is valid for any curvilinear coordinate systems. Its proof can be found in many standard textbooks on tensor analysis. Since we are still dealing with non-conical diffraction, in which the two fundamental polarization cases are decoupled, we can consider TM polarization only. It follows from (13.44)

$$\partial_3E_1-\partial_1E_3=\mathrm{i}k_0^*\mu H_2,\tag{13.45a}$$

$$\partial_1H_2=-\mathrm{i}k_0^*\varepsilon E^3,\tag{13.45b}$$

$$\partial_3H_2=\mathrm{i}k_0^*\varepsilon E^1,\tag{13.45c}$$

where $k_0^* = k_0\cos\zeta$ and we have used the fact that $H^2 = H_2$ for the particular coordinate system (13.35).

We now transform the equations in (13.45) into Fourier space while they are still in simple form. The modal field components are first expanded into Floquet-Fourier series, with an exponential x^3 dependence,

$$F(x^1, x^3) = \exp(\mathrm{i}\gamma x^3) \sum_{m=-\infty}^{\infty} F_m \exp(\mathrm{i}\alpha_m x^1), \tag{13.46}$$

where F stands for H_2, E_1, etc. The transformation of (13.45a) is straightforward, and that of (13.45c) requires using the inverse rule because E^1 is proportional to the component of **E** normal to the slanted sidewalls. The product εE^3 in (13.45b) is type 3 and requires some rearrangement. From (13.39)

$$E^1 = \frac{1}{\cos^2\zeta}(E_1 - \sin\zeta E_3), \tag{13.47a}$$

$$E^3 = E_3 - \sin\zeta E^1. \tag{13.47b}$$

Substitution of (13.47b) into (13.45b) allows Fourier factorization of the two terms using Laurent's rule and inverse rule separately. So, in Fourier space (13.45) becomes

$$\gamma E_1 - \boldsymbol{\alpha} E_3 = k_0^* \mu H_2, \tag{13.48a}$$

$$\boldsymbol{\alpha} H_2 = \frac{k_0}{\cos\zeta}\left[\sin\zeta \left[\!\left[\frac{1}{\varepsilon}\right]\!\right]^{-1} E_1 - \left(\left[\!\left[\varepsilon\right]\!\right]\cos^2\zeta + \left[\!\left[\frac{1}{\varepsilon}\right]\!\right]^{-1}\sin^2\zeta\right)E_3\right], \tag{13.48b}$$

$$\gamma H_2 = \frac{k_0}{\cos\zeta}\left[\!\left[\frac{1}{\varepsilon}\right]\!\right]^{-1}(E_1 - \sin\zeta E_3). \tag{13.48c}$$

In (13.48) H_2, E_1, and E_3 are understood as column vectors in Fourier space. Using (13.48b) to eliminate E_3 and after a little matrix algebraic manipulation we obtain

$$\begin{pmatrix} \left[\!\left[\frac{1}{\varepsilon}\right]\!\right]^{-1}\mathbf{G}\boldsymbol{\alpha}\sin\zeta & k_0^*\left[\!\left[\frac{1}{\varepsilon}\right]\!\right]^{-1}\mathbf{G}\left[\!\left[\varepsilon\right]\!\right] \\ \frac{k_0^*}{k_0^2}(k_0^2\mu\mathbf{I} - \boldsymbol{\alpha}\mathbf{G}\boldsymbol{\alpha}) & \sin\zeta\,\boldsymbol{\alpha}\mathbf{G}\left[\!\left[\frac{1}{\varepsilon}\right]\!\right]^{-1} \end{pmatrix}\begin{pmatrix} H_2 \\ E_1 \end{pmatrix} = \gamma\begin{pmatrix} H_2 \\ E_1 \end{pmatrix}, \tag{13.49}$$

where

$$\mathbf{G} = \left(\cos^2\zeta\left[\!\left[\varepsilon\right]\!\right] + \sin^2\zeta\left[\!\left[\frac{1}{\varepsilon}\right]\!\right]^{-1}\right)^{-1}. \tag{13.50}$$

Equation (13.49) is the matrix eigenvalue problem for the modal field of the slanted grating region. This equation consolidates Maxwell equations, the pseudo-periodicity condition, and the internal boundary conditions at the medium interfaces into one. Each of its solution vectors gives the Fourier coefficients of both field components needed for matching the external boundary conditions. The geometric interpretation of modal field in Fig. 13.2 obviously applies here. The only needed change is to rotate the infinite periodic medium and the modal field in it around the y axis clockwise by angle ζ.

To numerically solve (13.49) we need first to truncate the matrix, which can be done in the same way as for the rectangular grating case. If the Floquet-Fourier series are truncated from m_1 to $m_2 = N + m_1 - 1$, then the coefficient matrix in (13.49) is $2N \times 2N$, which is twice

as large as the one for a rectangular grating. Note that γ no longer appears as γ^2 in the eigenvalue equation, so the $2N$ eigenvalues in general do not form ± pairs. This may appear to contradict the intuition that inside the periodic layer modes propagating in both positive and negative directions of the x^3 axis are possible. The paradox is resolved when one realizes that a set of modes are determined subject to a pseudo-periodicity condition. Although in the un-slanted grating case both upward and downward modes share the same pseudo-periodicity condition, in the slanted grating case modes having eigenvalues of the same magnitude but opposite signs generally do not share the same pseudo-periodicity condition. Nevertheless the pseudo-periodicity condition is uniquely determined by the incident angle θ and the true grating period d.

To ensure that the S matrix algorithm work properly it is only necessary to partition the eigenvalue spectrum so that eigenvalues with positive imaginary parts are in set σ^+ and eigenvalues with negative imaginary parts are in set σ^-. (Here the superscripted σ is not to be confused with the tensor index σ.) The real eigenvalues can be arbitrarily distributed into σ^+ and σ^- as long as the two sets each contain N elements. This arbitrary handling is permissible because in an internal layer both upward and downward propagating and decay modes are present, and due to the boundedness of propagating modes misidentification of their propagation directions does not lead to any numerical error (a rigorous partition according to the true physical nature of the modes is possible, but troublesome and hardly necessary). The eigenvalues in $\sigma^\pm$ may be labeled by q, with $q = 1, 2, \ldots, N$, and sorted in ascending order of absolute values of imaginary parts.

After (13.49) is solved the total fields in the periodic layer can be written as

$$\begin{pmatrix} H_2(x^1,x^3) \\ E_1(x^1,x^3) \end{pmatrix} = \sum_{m=m_1}^{m_2} \exp(\mathrm{i}\alpha_m x^1) \sum_{q=1}^{N} \begin{pmatrix} H_{2mq}^+ & H_{2mq}^- \\ E_{1mq}^+ & E_{1mq}^- \end{pmatrix} \begin{pmatrix} \exp[\mathrm{i}\gamma_q^+(x^3-x_0^3)] & 0 \\ 0 & \exp[\mathrm{i}\gamma_q^-(x^3-x_1^3)] \end{pmatrix} \begin{pmatrix} \tilde{u}_q \\ \tilde{d}_q \end{pmatrix}, \tag{13.51}$$

where $\tilde{u}_q = u_q \exp(\mathrm{i}\gamma_q^+ x_0^3)$ and $\tilde{d}_q = d_q \exp(\mathrm{i}\gamma_q^- x_1^3)$ are the phase-adjusted unknown modal amplitudes, $x_0^3 = 0$, and $x_1^3 = \tilde{h}$. For later convenience, we also define $x_{-1}^3 = x_0^3$, $x_2^3 = x_1^3$.

13.2.3.4 Remaining steps

Solution of (13.51) gives both H_2 and E_1 that are needed for matching boundary conditions from the grating region side. In the homogeneous regions we have yet to find E_1. Since $E_1 = E^1 + \sin\zeta\, E^3$, it follows from (13.42) and (13.45)

$$E_1(x^1,x^3) = \frac{\gamma_0^{(2)-} - \alpha_0 \sin\zeta}{k_0^* \varepsilon^{(2)}} \exp(\mathrm{i}\alpha_0 x^1 + \mathrm{i}\gamma_0^{(2)-} x^3) + \frac{1}{k_0^* \varepsilon^{(2)}} \times$$

$$\times \sum_{m=-\infty}^{+\infty} (\gamma_m^{(2)+} - \alpha_m \sin\zeta) R_m^{(\mathrm{h})} \exp(\mathrm{i}\alpha_m x^1 + \mathrm{i}\gamma_m^{(2)+} x^3), \qquad x^3 \geq \tilde{h}; \tag{13.52a}$$

$$E_1(x^1,x^3) = \frac{1}{k_0^* \varepsilon^{(0)}} \sum_{m=-\infty}^{+\infty} (\gamma_m^{(0)-} - \alpha_m \sin\zeta) T_m^{(\mathrm{h})} \exp(\mathrm{i}\alpha_m x^1 + \mathrm{i}\gamma_m^{(0)-} x^3), \qquad x^3 \leq 0. \tag{13.52b}$$

From (13.42), (13.51), and (13.52) we obtain the **W** matrices in the same spirit as in Subsection 13.2.2.3,

$$\mathbf{W}^{(p)} = \begin{pmatrix} \delta_{mn} & \delta_{mn} \\ \dfrac{\gamma_m^{(p)+} - \alpha_m \sin\zeta}{k_0^* \varepsilon^{(p)}} \delta_{mn} & \dfrac{\gamma_m^{(p)-} - \alpha_m \sin\zeta}{k_0^* \varepsilon^{(p)}} \delta_{mn} \end{pmatrix}, \qquad p = 0, 2. \tag{13.53}$$

$$\mathbf{W}^{(1)} = \begin{pmatrix} H_{2mq}^{+} & H_{2mq}^{-} \\ E_{1mq}^{+} & E_{1mq}^{-} \end{pmatrix}. \tag{13.54}$$

These **W** matrices do not have the symmetry noted after (13.29). As illustrated in Subsection 13.2.2, after the **W** matrices are obtained, the grating problem is mostly solved. The matrix ϕ and vectors $\mathscr{F}$ and F can be defined similarly, using $\gamma_m^{(p)\pm}$ to replace $\pm\gamma_m^{(p)}$ and (x^1, x^3) to replace (x, z). After the resulting boundary matching equations are solved by using the S matrix algorithm, the Rayleigh amplitudes $R_m^{(\mathrm{h})}$ and $T_m^{(\mathrm{h})}$ are obtained. The diffraction efficiencies are given by

$$\eta_{m,\mathrm{TM}}^{(2)} = \frac{\gamma_m^{(2)+} - \alpha_m \sin\zeta}{\alpha_0 \sin\zeta - \gamma_0^{(2)-}} |R_m^{(\mathrm{h})}|^2, \qquad m \in U^{(2)}, \tag{13.55a}$$

$$\eta_{m,\mathrm{TM}}^{(0)} = \frac{\varepsilon^{(2)}}{\varepsilon^{(0)}} \cdot \frac{\alpha_m \sin\zeta - \gamma_m^{(0)-}}{\alpha_0 \sin\zeta - \gamma_0^{(2)-}} |T_m^{(\mathrm{h})}|^2, \qquad m \in U^{(0)}. \tag{13.55b}$$

13.3 One-dimensional gratings in conical mounting

13.3.1 Description of state of polarization of the incident and diffracted waves

When the wave vector $\mathbf{k}_{\mathrm{inc}}$ of an incident plane wave is in the principal plane of the grating all diffraction orders are also in the principal plane, and if the incident light is TE(TM) polarized, so are all diffracted orders. When $\mathbf{k}_{\mathrm{inc}}$ is not in the principal plane all diffracted orders fall on the side of a cone, whose axis is along the groove direction and whose cone angle is determined by the projection of $\mathbf{k}_{\mathrm{inc}}$ on the groove direction, hence the name conical mounting. It takes two angles to define $\mathbf{k}_{\mathrm{inc}}$. They are typically chosen as the polar angle θ formed by $\mathbf{k}_{\mathrm{inc}}$ with the grating normal and the azimuth angle ϕ that is the angle between the groove periodic direction and the projection of $\mathbf{k}_{\mathrm{inc}}$ on the grating plane (see Fig. 13.5 where the angle ϕ shown is positive). The ranges of θ and ϕ are $0 \le \theta < \pi/2$ and $-\pi < \phi \le \pi$, respectively. It is easy to verify that

$$\mathbf{k}_{\mathrm{inc}} = \mathbf{b}^1\alpha_0 + \mathbf{b}^2\beta_0 + \mathbf{b}^3\gamma_0^{(2)-}, \tag{13.56}$$

where

$$\alpha_0 = k^{(2)}\sin\theta\cos\phi, \quad \beta_0 = k^{(2)}\sin\theta\sin\phi, \quad \gamma_0^{(2)-} = \alpha_0\sin\zeta - k^{(2)}\cos\theta\cos\zeta. \tag{13.57}$$

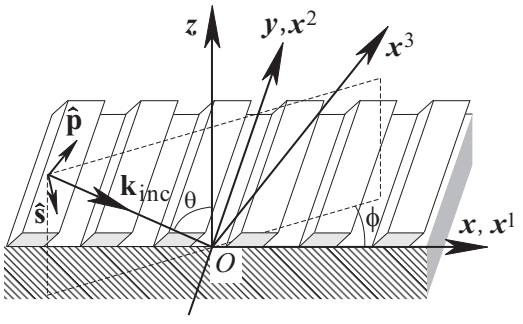

Fig. 13.5. Definition and notation of a slanted-grating problem in conical mounting.

The polarizations of the diffracted orders are in general elliptical even when the incident plane wave is linearly polarized. The polarization states of both incident and diffracted light in the two semi-infinite media can be fully specified in a number of ways. From a theoretical point of view the simplest is to use complex amplitudes of the y components of the electric and magnetic fields (the theoretical specification). From a practical point of view it is better to

define polarization with respect to a local reference frame $(\hat{\mathbf{p}}, \hat{\mathbf{s}}, \mathbf{k})$ that forms an orthogonal triplet with

$$\hat{\mathbf{s}} = \frac{\mathbf{k} \times \hat{\mathbf{z}}}{|\mathbf{k} \times \hat{\mathbf{z}}|}, \qquad \hat{\mathbf{p}} = \frac{\hat{\mathbf{s}} \times \mathbf{k}}{|\hat{\mathbf{s}} \times \mathbf{k}|}, \tag{13.58}$$

where $\mathbf{k}$ stands for the wave vector of the incident or a diffracted, reflected or transmitted plane wave. Due to transversality of the electromagnetic field of a plane wave in a homogeneous isotropic medium, the electric field vector of the incident or a diffracted order has this decomposition:

$$\mathbf{E} = (\mathbf{E} \cdot \hat{\mathbf{s}})\hat{\mathbf{s}} + (\mathbf{E} \cdot \hat{\mathbf{p}})\hat{\mathbf{p}} = E_{\mathrm{s}}\hat{\mathbf{s}} + E_{\mathrm{p}}\hat{\mathbf{p}}. \tag{13.59}$$

So, it suffices to know E_{s} and E_{p}, which are in general complex (the analytical specification). A more geometrical method is to use two angles (the analytic-geometric specification),

$$\alpha = \arctan\frac{|E_{\mathrm{s}}|}{|E_{\mathrm{p}}|}, \qquad \delta = \arg\frac{E_{\mathrm{p}}}{E_{\mathrm{s}}}. \tag{13.60}$$

The fully geometric specification is to use the orientation angle ψ of the major axis of the polarization ellipse with respect to the p axis and the ellipticity angle

$$\chi = \pm\arctan\frac{b}{a}, \tag{13.61}$$

where the a and b are the lengths the major and minor axes of the polarization ellipse, respectively, and the ± signs distinguish between right-handed and left-handed waves. It is elementary to convert from one specification to another one, typically from analytic-geometric or geometric one to theoretic one for the incident plane wave and in the reverse direction for the calculated diffracted waves.

In any case, it is recommended to use the (p, s) reference to describe polarization state for conical mountings and to reserve TE or TM for non-conical mounting.

13.3.2 Isotropic gratings

The Fourier modal method has been applied by several authors to treat rectangular gratings in conical mounting, but to date a complete and fully correct formulation is still unpublished. The method has also been applied to slanted volume gratings or parallelogram gratings [13.15, 13.16]; however, the presented formulations are inefficient because the rectangular Cartesian coordinate system is used and the size of the derived matrix eigenvalue problem is twice as large as it could be. In this section we continue to deal with slanted gratings. An efficient formulation that uses the minimum matrix size is derived in the matched oblique coordinate system. A full set of formulas for the un-slanted grating problem are given as a special case.

13.3.2.1 Rayleigh expansions in oblique coordinates and conical mounting

In conical mounting Rayleigh expansions are still available in the two semi-infinite homogenous media. Since the grating structure is invariant in the y direction, an exponential y dependence is shared by all field components and it is convenient to work with the y components of the fields. It is easy to show that

$$E_2(x^1, x^2, x^3) = I^{(\mathrm{e})} \exp[\mathrm{i}(\alpha_0 x^1 + \beta_0 x^2 + \gamma_0^{(2)-} x^3)] + \\ + \sum_{m=-\infty}^{+\infty} R_m^{(\mathrm{e})} \exp[\mathrm{i}(\alpha_m x^1 + \beta_0 x^2 + \gamma_m^{(2)+} x^3)], \qquad x^3 \geq \tilde{h}; \tag{13.62a}$$

$$E_2(x^1,x^2,x^3)=\sum_{m=-\infty}^{+\infty} T_m^{(\mathrm{e})}\exp[\mathrm{i}(\alpha_m x^1+\beta_0 x^2+\gamma_m^{(0)-}x^3)], \qquad x^3\le 0. \tag{13.62b}$$

$$H_2(x^1,x^2,x^3)=I^{(\mathrm{h})}\exp[\mathrm{i}(\alpha_0 x^1+\beta_0 x^2+\gamma_0^{(2)-}x^3)]+ \\ +\sum_{m=-\infty}^{+\infty} R_m^{(\mathrm{h})}\exp[\mathrm{i}(\alpha_m x^1+\beta_0 x^2+\gamma_m^{(2)+}x^3)], \qquad x^3\ge \tilde{h}; \tag{13.63a}$$

$$H_2(x^1,x^2,x^3)=\sum_{m=-\infty}^{+\infty} T_m^{(\mathrm{h})}\exp[\mathrm{i}(\alpha_m x^1+\beta_0 x^2+\gamma_m^{(0)-}x^3)], \qquad x^3\le 0. \tag{13.63b}$$

where

$$\gamma_m^{(p)\pm}=\alpha_m\sin\zeta\pm\sqrt{\tilde{k}^{(p)2}-\alpha_m^2}\,\cos\zeta, \\ \tilde{k}^{(p)2}=k^{(p)2}-\beta_0^2, \qquad \mathrm{Re}[\sqrt{\tilde{k}^{(p)2}-\alpha_m^2}\,]+\mathrm{Im}[\sqrt{\tilde{k}^{(p)2}-\alpha_m^2}\,]>0, \qquad p=0,2, \tag{13.64}$$

and $I^{(\mathrm{e})}$ and $I^{(\mathrm{h})}$ are the y components of the incident electric and magnetic vectors, respectively. Evidently here $\tilde{k}^{(p)2}$ plays the role that $k^{(p)2}$ plays in (13.43). The arguments of exponential functions in the Rayleigh expansions can be written as

$$\mathrm{i}\mathbf{k}_m^{(p)\pm}\cdot\mathbf{r}=\mathrm{i}(\alpha_m\mathbf{b}^1+\beta_0\mathbf{b}^2+\gamma_m^{(p)\pm}\mathbf{b}^3)\cdot(\mathbf{b}_1x^1+\mathbf{b}_2x^2+\mathbf{b}_3x^3). \tag{13.65}$$

Therefore, α_m, β_0, and $\gamma_m^{(p)\pm}$ are the first, second, and third covariant components of the mth diffracted wave vector $\mathbf{k}_m^{(p)\pm}$, respectively.

13.3.2.2 Minimum-matrix-size eigenvalue problem

The key to achieving a minimum-matrix-size formulation is to make decomposition of the fields in the periodic layer according to two characteristic polarization states. Since the modes of the periodic region are sought as if the region is infinite in the vertical direction, the geometric modal picture of Fig. 13.2 is still valid. As is remarked a few lines below (13.50) a rotation of the picture about the y axis to fit the coordinate system of Fig. 13.5 is needed. However, a major difference takes place here. In conical mounting the plane of the zigzag paths of a mode is still perpendicular to the slanted medium interfaces but it is no longer perpendicular to the y axis. It is rotated around the vector $\mathbf{b}^1$ of Fig. 13.4 by an angle such that the projection of the wave vectors on the y axis is β_0. Since β_0 is a constant and the zigzag angles depend on both the mode order number and polarization, so does this rotation angle. Therefore, a nonzero β_0 results in two sets of infinitely many planes of zigzag paths. Within one set the electric field vector of a mode is along the normal of its associated zigzag plane, and within the other set the magnetic field vector is along the normal. Although the normal vectors of the zigzag planes are different, they have one feature in common: they are all perpendicular to $\mathbf{b}^1$. If we recall the geometric interpretation of contravariant components of a vector, we can say that in the case of conical mounting the modes within the periodic region are characterized by $E^1 = 0$ and $H^1 = 0$. A mode with $E^1 = 0$ will be called an $E_\perp$ mode and denoted by a superscript (e), and a mode with $H^1 = 0$ will be called an $H_\perp$ mode and denoted by a superscript (h). In a conical diffraction problem both polarization modes are excited and any field inside the periodic medium can be decomposed into a superposition of $E_\perp$ modes and $H_\perp$ modes.

From Maxwell equations it can be shown that in a medium with ε such that $\partial_2\varepsilon = \partial_3\varepsilon = 0$, the second covariant component of magnetic field vector of an $H_\perp$ mode obeys equation

$$\varepsilon\,\partial_\rho \frac{1}{\varepsilon} g^{\rho\sigma}\partial_\sigma H_2^{(\mathrm{h})} + \varepsilon\mu k_0^2 H_2^{(\mathrm{h})} = 0. \tag{13.66}$$

After expansion and rearrangement for the purpose of Fourier factorization it becomes

$$\varepsilon\left[\mu k_0^2 + \frac{1}{\cos^2\zeta}(\partial_1 - \sin\zeta\,\partial_3)\frac{1}{\varepsilon}(\partial_1 - \sin\zeta\,\partial_3)\right]H_2^{(\mathrm{h})} + (\partial_2^2 + \partial_3^2)H_2^{(\mathrm{h})} = 0. \tag{13.67}$$

In the next subsection we will see that $(1/\varepsilon)(\partial_1 - \sin\zeta\,\partial_3)H_2$ is proportional to E_3; therefore, similar to the treatment of (13.17), for both appearances of ε in (13.67) the inverse rule should be used. With an exponential dependence $\exp(\mathrm{i}\beta_0 x^2 + \mathrm{i}\gamma x^3)$ for the modal fields, (13.67) becomes

$$\begin{aligned}&\left[\cos^2\zeta\left(\mu k_0^2\mathbf{I} - \beta_0^2\left[\!\left[\frac{1}{\varepsilon}\right]\!\right]\right) - \boldsymbol{\alpha}[\![\varepsilon]\!]^{-1}\boldsymbol{\alpha}\right]H_2^{(\mathrm{h})} + \\ &+ \gamma\sin\zeta\left([\![\varepsilon]\!]^{-1}\boldsymbol{\alpha} + \boldsymbol{\alpha}[\![\varepsilon]\!]^{-1}\right)H_2^{(\mathrm{h})} - \gamma^2\left(\cos^2\zeta\left[\!\left[\frac{1}{\varepsilon}\right]\!\right] + \sin^2\zeta\,[\![\varepsilon]\!]^{-1}\right)H_2^{(\mathrm{h})} = 0,\end{aligned} \tag{13.68}$$

which is a quadratic equation in γ. Suppose the column vector $H_2^{(\mathrm{h})}$ is truncated to be $N \times 1$, then to turn the equation into a standard matrix eigenvalue problem it is necessary to double the length of the eigenvector. There are a number of ways to do this and perhaps the simplest way is to let $(\gamma H_2^{(\mathrm{h})}, H_2^{(\mathrm{h})})^{\mathrm{T}}$ be the enlarged vector. Then (13.68) is equivalent to

$$\begin{aligned}&\begin{pmatrix}\mathbf{Q}\sin\zeta\left(\boldsymbol{\alpha}[\![\varepsilon]\!]^{-1} + [\![\varepsilon]\!]^{-1}\boldsymbol{\alpha}\right) & \mathbf{Q}\left[\cos^2\zeta\left(\mu k_0^2\mathbf{I} - \beta_0^2\left[\!\left[\frac{1}{\varepsilon}\right]\!\right]\right) - \boldsymbol{\alpha}[\![\varepsilon]\!]^{-1}\boldsymbol{\alpha}\right]\\ \mathbf{I} & 0\end{pmatrix}\begin{pmatrix}\gamma H_2^{(\mathrm{h})}\\ H_2^{(\mathrm{h})}\end{pmatrix}\\ &= \gamma\begin{pmatrix}\gamma H_2^{(\mathrm{h})}\\ H_2^{(\mathrm{h})}\end{pmatrix}, \qquad \mathbf{Q} = \left(\cos^2\zeta\left[\!\left[\frac{1}{\varepsilon}\right]\!\right] + \sin^2\zeta\,[\![\varepsilon]\!]^{-1}\right)^{-1}.\end{aligned} \tag{13.69}$$

The matrix eigenvalue problem for an $E_\perp$ mode can be obtained by using the electromagnetic symmetry. Making the change $H_2^{(\mathrm{h})} \to E_2^{(\mathrm{e})}$ and exchange $\varepsilon \leftrightarrow -\mu$ in (13.69) and using the fact that μ is a constant we get

$$\begin{pmatrix}2\sin\zeta\,\boldsymbol{\alpha} & \cos^2\zeta\,(\mu k_0^2[\![\varepsilon]\!] - \beta_0^2) - \boldsymbol{\alpha}^2\\ \mathbf{I} & 0\end{pmatrix}\begin{pmatrix}\gamma E_2^{(\mathrm{e})}\\ E_2^{(\mathrm{e})}\end{pmatrix} = \gamma\begin{pmatrix}\gamma E_2^{(\mathrm{e})}\\ E_2^{(\mathrm{e})}\end{pmatrix}. \tag{13.70}$$

The use of $[\![\varepsilon]\!]$ in the above is justified because ε is multiplied by $E_2^{(\mathrm{e})}$, a continuous quantity. The size of the matrix eigenvalue problems in (13.69) and (13.70) are both $2N \times 2N$. The computation time to solve each of them is about 1/8 of the time needed to solve the $4N \times 4N$ matrix eigenvalue problems in the previously published formulations of the slanted gratings in conical mountings. Since both $E_\perp$ and $H_\perp$ modes are needed for matching boundary conditions, the overall time saving factor is 1/4.

The eigenvalue spectra $\sigma^{(\mathrm{e})}$ of the $E_\perp$ modes and $\sigma^{(\mathrm{h})}$ of the $H_\perp$ modes are to be partitioned separately in the same way as explained in Subsection 13.2.3.3. Besides the superscripts ± and subscript $q = 1, 2, \ldots, N$, the eigenvalues will be superscripted with (e) and (h). Altogether we have $4N$ eigen-solutions. Note that for a fixed q, $\gamma_q^{(\mathrm{e})\pm}$ is not related to $\gamma_q^{(\mathrm{h})\pm}$ although they have the same subscript q.

13.3.2.3 Construction of the total fields

In a conical diffraction problem four vector components of the electromagnetic fields, E_2, H_2, E_1, and H_1, are needed to match the boundary conditions between two adjacent spatial regions. Both $E_\perp$ and $H_\perp$ modes contribute to these four field components, so we need eight sub-components: $E_2^{(\mathrm{e})}$, $H_2^{(\mathrm{h})}, E_2^{(\mathrm{h})}$, $H_2^{(\mathrm{e})}, E_1^{(\mathrm{e})}$, $H_1^{(\mathrm{h})}, E_1^{(\mathrm{h})}$, and $H_1^{(\mathrm{e})}$. The first two are already given as solutions to (13.69) and (13.70). The others can be expressed in terms of the first two as follows.

In a waveguide or diffraction structure that is invariant along a Cartesian coordinate axis, such as the x^2 axis in Fig. 13.5, the transverse components of the electromagnetic field vectors can be expressed in terms of their longitudinal components. In our present oblique coordinate system

$$H^1 = \frac{\mathrm{i}}{\tilde{k}^2}\left(\beta_0 g^{1\tau}\partial_\tau H_2 + \frac{k_0\varepsilon}{\sqrt{g}}\partial_3 E_2\right). \tag{13.71}$$

$$E_3 = \frac{\mathrm{i}}{\tilde{k}^2}\left(\beta_0\partial_3 E_2 + k_0\mu\sqrt{g}\, g^{3\tau}\partial_\tau H_2\right). \tag{13.72}$$

Then, for any $H_\perp$ field it immediately follows that

$$\partial_3 E_2^{(\mathrm{h})} = -\frac{\beta_0}{k_0^*\varepsilon}(\partial_1 - \sin\zeta\,\partial_3) H_2^{(\mathrm{h})}. \tag{13.73}$$

Substituting (13.73) into (13.72) gives

$$E_3^{(\mathrm{h})} = \frac{\mathrm{i}}{k_0^*\varepsilon}(\partial_1 - \sin\zeta\,\partial_3) H_2^{(\mathrm{h})}. \tag{13.74}$$

Since $E_3^{(\mathrm{h})}$ is continuous Fourier transforming (13.73) leads to

$$E_{2q}^{(\mathrm{h})} = -\frac{\beta_0}{k_0^*\gamma_q^{(\mathrm{h})}}[\![\varepsilon]\!]^{-1}(\boldsymbol{\alpha} - \gamma_q^{(\mathrm{h})}\sin\zeta)\, H_{2q}^{(\mathrm{h})}. \tag{13.75a}$$

This equation is valid for a mode, as indicated by the attached subscript q to the eigenvalue and the field components. Next, $E_1^{(\mathrm{e})}$ can be obtained by using (13.47) and equation $\nabla\cdot\mathbf{D} = 0$. The former gives $E_1^{(\mathrm{e})} = \sin\zeta E_3^{(\mathrm{e})}$ and $E_3^{(\mathrm{e})} = E^{3(\mathrm{e})}$, and the latter can be expanded as

$$\varepsilon\nabla\cdot\mathbf{E}^{(\mathrm{e})} + (\nabla\varepsilon)\cdot\mathbf{E}^{(\mathrm{e})} = \varepsilon\partial_\sigma E^{\sigma(\mathrm{e})} + (\partial_1\varepsilon)E^{1(\mathrm{e})} = \partial_2 E^{2(\mathrm{e})} + \partial_3 E^{3(\mathrm{e})} = \partial_2 E_2^{(\mathrm{e})} + \partial_3 E_3^{(\mathrm{e})} = 0. \tag{13.76}$$

It then follows that

$$E_{1q}^{(\mathrm{e})} = -\frac{\beta_0}{\gamma_q^{(\mathrm{e})}}\sin\zeta\, E_{2q}^{(\mathrm{e})}. \tag{13.77a}$$

Finally, $E_1^{(\mathrm{h})}$ can be obtained by using (13.45a) and (13.74). The result is

$$E_{1q}^{(\mathrm{h})} = \frac{1}{k_0^*\gamma_q^{(\mathrm{h})}}\left[\mu k_0^2\cos^2\zeta - \boldsymbol{\alpha}[\![\varepsilon]\!]^{-1}(\boldsymbol{\alpha} - \gamma_q^{(\mathrm{h})}\sin\zeta)\right] H_{2q}^{(\mathrm{h})}. \tag{13.78a}$$

From the electromagnetic symmetry the magnetic images of (13.75a), (13.77a) and (13.78a) are

$$H_{2q}^{(\mathrm{e})} = \frac{\beta_0}{k_0^* \mu \gamma_q^{(\mathrm{e})}} (\boldsymbol{\alpha} - \gamma_q^{(\mathrm{e})} \sin\zeta)\, E_{2q}^{(\mathrm{e})}, \tag{13.75b}$$

$$H_{1q}^{(\mathrm{h})} = -\frac{\beta_0}{\gamma_q^{(\mathrm{h})}} \sin\zeta\, H_{2q}^{(\mathrm{h})}, \tag{13.77b}$$

$$H_{1q}^{(\mathrm{e})} = \frac{-1}{k_0^* \mu \gamma_q^{(\mathrm{e})}} \Big[\mu k_0^2 \cos^2\zeta \, [\![\varepsilon]\!] - \boldsymbol{\alpha} (\boldsymbol{\alpha} - \gamma_q^{(\mathrm{e})} \sin\zeta) \Big] E_{2q}^{(\mathrm{e})}. \tag{13.78b}$$

Collecting all of the above expressions of the sub-components of the fields we have

$$\mathscr{F}(x^3) = \mathbf{W}^{(1)}\, \phi(x^3)\, F, \tag{13.79}$$

where

$$\mathscr{F} = (E_{2m}, H_{2m}, H_{1m}, E_{1m})^{\mathrm{T}}, \qquad F = (\tilde{u}_q^{(\mathrm{e})}, \tilde{u}_q^{(\mathrm{h})}, \tilde{d}_q^{(\mathrm{e})}, \tilde{d}_q^{(\mathrm{h})})^{\mathrm{T}}, \tag{13.80}$$

$$\mathbf{W}^{(1)} = \begin{pmatrix} E_{2mq}^{(\mathrm{e})+} & -\beta_0 V_{mq}^{(\mathrm{h})+} & E_{2mq}^{(\mathrm{e})-} & -\beta_0 V_{mq}^{(\mathrm{h})-} \\ \beta_0 V_{mq}^{(\mathrm{e})+} & H_{2mq}^{(\mathrm{h})+} & \beta_0 V_{mq}^{(\mathrm{e})-} & H_{2mq}^{(\mathrm{h})-} \\ -U_{mq}^{(\mathrm{e})+} & -B_q^{(\mathrm{h})+} H_{2mq}^{(\mathrm{h})+} & -U_{mlq}^{(\mathrm{e})-} & -B_q^{(\mathrm{h})-} H_{2mq}^{(\mathrm{h})-} \\ -B_q^{(\mathrm{e})+} E_{2mq}^{(\mathrm{e})+} & U_{mq}^{(\mathrm{h})+} & -B_q^{(\mathrm{e})-} E_{2mq}^{(\mathrm{e})-} & U_{mlq}^{(\mathrm{h})-} \end{pmatrix}, \tag{13.81}$$

$$\phi^{(1)} = \begin{pmatrix} \exp[\mathrm{i}\gamma_q^{(\mathrm{e})+}(x^3 - x_0^3)] & 0 & 0 & 0 \\ 0 & \exp[\mathrm{i}\gamma_q^{(\mathrm{h})+}(x^3 - x_0^3)] & 0 & 0 \\ 0 & 0 & \exp[\mathrm{i}\gamma_q^{(\mathrm{e})-}(x^3 - x_1^3)] & 0 \\ 0 & 0 & 0 & \exp[\mathrm{i}\gamma_q^{(\mathrm{h})-}(x^3 - x_1^3)] \end{pmatrix}. \tag{13.82}$$

Note that in (13.80) H_{1m} is listed before E_{1m} in $\mathscr{F}$ and the modal amplitudes in F are phase-adjusted in a way similar to that in (13.24) and (13.32). In (13.81)

$$V_{mq}^{(\mathrm{e})\pm} = \frac{1}{k_0^* \mu \gamma_q^{(\mathrm{e})\pm}} \left(\alpha_m - \gamma_q^{(\mathrm{e})\pm} \sin\zeta \right) E_{2mq}^{(\mathrm{e})\pm}, \tag{13.83a}$$

$$V_{mq}^{(\mathrm{h})\pm} = \frac{1}{k_0^* \gamma_q^{(\mathrm{h})\pm}} \sum_{n=m_1}^{m_2} [\![\varepsilon]\!]_{mn}^{-1} \left(\alpha_n - \gamma_q^{(\mathrm{h})\pm} \sin\zeta \right) H_{2nq}^{(\mathrm{h})\pm}, \tag{13.83b}$$

$$U_{mq}^{(\mathrm{e})\pm} = \frac{k_0^*}{\gamma_q^{(\mathrm{e})\pm}} \sum_{n=m_1}^{m_2} [\![\varepsilon]\!]_{mn} E_{2nq}^{(\mathrm{e})\pm} - \alpha_m V_{mq}^{(\mathrm{e})\pm}, \tag{13.84a}$$

$$U_{mq}^{(\mathrm{h})\pm} = \frac{k_0^* \mu}{\gamma_q^{(\mathrm{h})\pm}} H_{2mq}^{(\mathrm{h})\pm} - \alpha_m V_{mq}^{(\mathrm{h})\pm}, \tag{13.84b}$$

$B_q^{(s)\pm} = \beta_0 \sin\zeta / \gamma_q^{(s)\pm}$, and s = e, h. Using (13.69) and (13.70), (13.84) can be written in another way

$$U_{mq}^{(\mathrm{e})\pm} = \frac{1}{k_0^* \mu \gamma_q^{(\mathrm{e})\pm}} \Big[\cos^2\zeta\, \beta_0^2 + (\gamma_q^{(\mathrm{e})\pm})^2 - \gamma_q^{(\mathrm{e})\pm} \sin\zeta\, \alpha_m \Big] E_{2mq}^{(\mathrm{e})\pm}, \tag{13.85a}$$

$$U_{mq}^{(\mathrm{h})\pm}=\frac{1}{k_0^*\gamma_q^{(\mathrm{h})\pm}}\sum_{n=m_1}^{m_2}\left[\left(\cos^2\zeta\,\beta_0^2\left[\!\left[\frac{1}{\varepsilon}\right]\!\right]+(\gamma_q^{(\mathrm{h})\pm})^2\mathbf{Q}^{-1}\right)_{mn}-\gamma_q^{(\mathrm{h})\pm}\sin\zeta\left(\left[\!\left[\varepsilon\right]\!\right]^{-1}\right)_{mn}\alpha_n\right]H_{2nq}^{(\mathrm{h})\pm}. \quad (13.85b)$$

A comparison between (13.84) and (13.85) shows that it is simpler to use (13.85a) to compute $U_{mq}^{(\mathrm{e})\pm}$ and to use (13.84b) to compute $U_{mq}^{(\mathrm{h})\pm}$.

From (13.62) and (13.63) the Rayleigh expansions of E_1 and H_1 in the homogeneous regions can be derived from Maxwell equations,

$$E_1=[-\tau_3^{(2)}\alpha_0 I^{(\mathrm{e})}+\tau_2^{(2)}(\gamma_0^{(2)-}-\alpha_0\sin\zeta)I^{(\mathrm{h})}]\exp[\mathrm{i}(\alpha_0 x^1+\beta_0 x^2+\gamma_0^{(2)-}x^3)]+$$
$$+\sum_{m=-\infty}^{+\infty}[-\tau_3^{(2)}\alpha_m R_m^{(\mathrm{e})}+\tau_2^{(2)}(\gamma_m^{(2)+}-\alpha_m\sin\zeta)R_m^{(\mathrm{h})}]\exp[\mathrm{i}(\alpha_m x^1+\beta_0 x^2+\gamma_m^{(2)+}x^3)],$$
$$x^3\ge\tilde{h}; \quad (13.86a)$$

$$E_1=\sum_{m=-\infty}^{+\infty}[-\tau_3^{(0)}\alpha_m T_m^{(\mathrm{e})}+\tau_2^{(0)}(\gamma_m^{(0)-}-\alpha_m\sin\zeta)T_m^{(\mathrm{h})}]\exp[\mathrm{i}(\alpha_m x^1+\beta_0 x^2+\gamma_m^{(0)-}x^3)],$$
$$x^3\le 0; \quad (13.86b)$$

$$H_1=[-\tau_3^{(2)}\alpha_0 I^{(\mathrm{h})}-\tau_1^{(2)}(\gamma_0^{(2)-}-\alpha_0\sin\zeta)I^{(\mathrm{e})}]\exp[\mathrm{i}(\alpha_0 x^1+\beta_0 x^2+\gamma_0^{(2)-}x^3)]+$$
$$+\sum_{m=-\infty}^{+\infty}[-\tau_3^{(2)}\alpha_m R_m^{(\mathrm{h})}-\tau_1^{(2)}(\gamma_m^{(2)+}-\alpha_m\sin\zeta)R_m^{(\mathrm{e})}]\exp[\mathrm{i}(\alpha_m x^1+\beta_0 x^2+\gamma_m^{(2)+}x^3)],$$
$$x^3\ge\tilde{h}; \quad (13.87a)$$

$$H_1=\sum_{m=-\infty}^{+\infty}[-\tau_3^{(0)}\alpha_m T_m^{(\mathrm{h})}-\tau_1^{(0)}(\gamma_m^{(0)-}-\alpha_m\sin\zeta)T_m^{(\mathrm{e})}]\exp(\mathrm{i}\alpha_m x^1+\mathrm{i}\beta_0 x^2+\mathrm{i}\gamma_m^{(0)-}x^3),$$
$$x^3\le 0, \quad (13.87b)$$

where

$$\tau_1^{(p)}=\frac{k_0\varepsilon^{(p)}}{\tilde{k}^{(p)2}\cos\zeta}, \qquad \tau_2^{(p)}=\frac{k_0\mu^{(p)}}{\tilde{k}^{(p)2}\cos\zeta}, \qquad \tau_3^{(p)}=\frac{\beta_0}{\tilde{k}^{(p)2}}. \quad (13.88)$$

With these results we can write down the counterparts of the right-hand side of (13.79) for the homogeneous regions:

$$F^{(2)}=(\tilde{R}_m^{(\mathrm{e})},\tilde{R}_m^{(\mathrm{h})},\tilde{I}^{(\mathrm{e})}\delta_{m0},\tilde{I}^{(\mathrm{h})}\delta_{m0})^{\mathrm{T}}, \qquad F^{(0)}=(0,0,\tilde{T}_m^{(\mathrm{e})},\tilde{T}_m^{(\mathrm{h})})^{\mathrm{T}}, \quad (13.89)$$

$$\mathbf{W}^{(p)}=\begin{pmatrix}\delta_{mn} & 0 & \delta_{mn} & 0\\ 0 & \delta_{mn} & 0 & \delta_{mn}\\ -\tau_1^{(p)}\Gamma_m^{(p)+}\delta_{mn} & -\tau_3^{(p)}\alpha_m\delta_{mn} & -\tau_1^{(p)}\Gamma_m^{(p)-}\delta_{mn} & -\tau_3^{(p)}\alpha_m\delta_{mn}\\ -\tau_3^{(p)}\alpha_m\delta_{mn} & \tau_2^{(p)}\Gamma_m^{(p)+}\delta_{mn} & -\tau_3^{(p)}\alpha_m\delta_{mn} & \tau_2^{(p)}\Gamma_m^{(p)-}\delta_{mn}\end{pmatrix}, \quad p=0,2, \quad (13.90)$$

$$\phi^{(p)}=\begin{pmatrix}\exp(\mathrm{i}\gamma_m^{(p)+}x^3) & 0 & 0 & 0\\ 0 & \exp(\mathrm{i}\gamma_m^{(p)+}x^3) & 0 & 0\\ 0 & 0 & \exp(\mathrm{i}\gamma_m^{(p)-}x^3) & 0\\ 0 & 0 & 0 & \exp(\mathrm{i}\gamma_m^{(p)-}x^3)\end{pmatrix}, \quad p=0,2, \quad (13.91)$$

where $\Gamma_m^{(p)\pm} = \gamma_m^{(p)\pm} - \alpha_m \sin\zeta$, and $\tilde{R}_m^{(\mathrm{e})}, \tilde{R}_m^{(\mathrm{h})}$, etc. are phase adjusted as in (13.25).

Using (13.62), (13.63), (13.86), and (13.87), from the basic definition of diffraction efficiency one can derive the diffraction efficiencies of reflected and transmitted orders in conical mounting

$$\eta_m^{(2)} = \frac{\gamma_m^{(2)+} - \alpha_m \sin\zeta}{\alpha_0 \sin\zeta - \gamma_0^{(2)-}} \cdot \frac{\varepsilon^{(2)} |R_m^{(\mathrm{e})}|^2 + \mu |R_m^{(\mathrm{h})}|^2}{\varepsilon^{(2)} |I^{(\mathrm{e})}|^2 + \mu |I^{(\mathrm{h})}|^2}, \qquad m \in U^{(2)}, \tag{13.92a}$$

$$\eta_m^{(0)} = \frac{\tilde{k}^{(2)2}}{\tilde{k}^{(0)2}} \cdot \frac{\alpha_m \sin\zeta - \gamma_m^{(0)-}}{\alpha_0 \sin\zeta - \gamma_0^{(2)-}} \cdot \frac{\varepsilon^{(0)} |T_m^{(\mathrm{e})}|^2 + \mu |T_m^{(\mathrm{h})}|^2}{\varepsilon^{(2)} |I^{(\mathrm{e})}|^2 + \mu |I^{(\mathrm{h})}|^2}, \qquad m \in U^{(0)}. \tag{13.92b}$$

The two Rayleigh amplitudes $R_m^{(\mathrm{e})}$ and $R_m^{(\mathrm{h})}$ fully specify the state of polarization of the mth reflected order. To convert this specification to the analytic-geometric specification one can take the following steps. Since $R_m^{(\mathrm{e})}$ stands for E_2 and E_1 is already given in (13.86), to complete the information about **E**, E_3 can be obtained by using transversality of plane wave, $\mathbf{k} \cdot \mathbf{E} = k_\rho g^{\rho\sigma} E_\sigma = 0$, where $k_1 = \alpha_m$, $k_2 = \beta_0$, and $k_3 = \gamma_m^{(p)\pm}$. The local reference frame $(\hat{\mathbf{p}}, \hat{\mathbf{s}}, \mathbf{k})$ can be established once **k** is known. Then, E_s and E_p can be easily obtained from (13.58) and (13.59).

The previous formulations of slanted gratings in conical mounting output all four tangential components of the electromagnetic fields needed for matching boundary conditions as eigenvectors of a $4N \times 4N$ eigenvalue problem, so the **W** matrix is built automatically except sorting of eigenvalues. In the present formulation after the eigenvectors are obtained some work is needed to build the **W** matrix. However, this additional work is insignificant compared with the saving gained by solving two $2N \times 2N$ eigenvalue problems.

13.3.2.4 Special cases of rectangular gratings and non-conical mounting

For rectangular isotropic gratings in conical mounting all required formulas can be obtained by setting $\zeta = 0$ in Subsections 13.3.2.1-3.2.3. In particular, it follows from (13.69) and (13.70) the $H_\perp$ and $E_\perp$ modes can be solved from two simpler equations

$$\left[\!\left[\frac{1}{\varepsilon}\right]\!\right]^{-1} \left(k_0^2 \mu \mathbf{I} - \boldsymbol{\alpha} \left[\!\left[\varepsilon\right]\!\right]^{-1} \boldsymbol{\alpha} \right) H_2^{(\mathrm{h})} = (\gamma^2 + \beta_0^2) H_2^{(\mathrm{h})}, \tag{13.93a}$$

$$\left(k_0^2 \mu \left[\!\left[\varepsilon\right]\!\right] - \boldsymbol{\alpha}^2 \right) E_2^{(\mathrm{e})} = (\gamma^2 + \beta_0^2) E_2^{(\mathrm{e})}. \tag{13.93b}$$

The difference between (13.93a) and (13.18) is only in the eigenvalues. The $\mathbf{W}^{(1)}$ matrix for the grating layer becomes

$$\mathbf{W}^{(1)} = \begin{pmatrix} E_{2mq}^{(\mathrm{e})+} & -\tilde{V}_{mq}^{(\mathrm{h})+} & E_{2mq}^{(\mathrm{e})-} & -\tilde{V}_{mq}^{(\mathrm{h})-} \\ \tilde{V}_{mq}^{(\mathrm{e})+} & H_{2mq}^{(\mathrm{h})+} & \tilde{V}_{mq}^{(\mathrm{e})-} & H_{2mq}^{(\mathrm{h})-} \\ -\tilde{U}_{mq}^{(\mathrm{e})+} & 0 & -\tilde{U}_{mq}^{(\mathrm{e})-} & 0 \\ 0 & \tilde{U}_{mq}^{(\mathrm{h})+} & 0 & \tilde{U}_{mlq}^{(\mathrm{h})-} \end{pmatrix}, \tag{13.94}$$

where

$$\tilde{V}_{mq}^{(\mathrm{e})\pm} = \frac{\beta_0 \alpha_m}{k_0 \mu \gamma_q^{(\mathrm{e})\pm}} E_{2mq}^{(\mathrm{e})\pm}, \qquad \tilde{U}_{mq}^{(\mathrm{e})\pm} = \frac{\beta_0^2 + (\gamma_q^{(\mathrm{e})\pm})^2}{k_0 \mu \gamma_q^{(\mathrm{e})\pm}} E_{2mq}^{(\mathrm{e})\pm}, \tag{13.95a}$$

$$\tilde{V}_{mq}^{(\mathrm{h})\pm} = \frac{\beta_0}{k_0 \gamma_q^{(\mathrm{h})\pm}} \sum_{n=m_1}^{m_2} [\![\varepsilon]\!]_{mn}^{-1} \alpha_n H_{2nq}^{(\mathrm{h})\pm}, \quad \tilde{U}_{mq}^{(\mathrm{h})\pm} = \frac{\beta_0^2 + (\gamma_q^{(\mathrm{h})\pm})^2}{k_0 \gamma_q^{(\mathrm{h})\pm}} \sum_{n=m_1}^{m_2} \left[\!\!\left[\frac{1}{\varepsilon}\right]\!\!\right]_{mn} H_{2nq}^{(\mathrm{h})\pm}. \tag{13.95b}$$

The $\mathbf{W}^{(p)}$ matrices for $p = 0$ and 2 can be obtained from (13.90) by simply replacing $\Gamma_m^{(p)\pm}$ with $\gamma_m^{(p)\pm}$. Equations (13.94) and (13.95) can be compared with equations (61-65) of [13.3]. Evidently, to prepare Fourier coefficient of the total fields needed for matching boundary conditions between the periodic region and the homogeneous regions, the present formulation requires much less matrix computation.

By setting $\beta_0 = 0$ in (13.69), (13.70), (13.81), and (13.90) we obtain an alternative formulation of the Fourier modal method for slanted gratings in classical mounting. The eigenvalue problems for both TM and TE polarizations are still $2N \times 2N$, as long as the slant angle ζ is nonzero. After row exchange $2 \leftrightarrow 3$ and column exchange $2 \leftrightarrow 3$, the 4×4 $\mathbf{W}^{(p)}$ matrices become 2×2 block-diagonal; therefore, TM and TE polarizations are uncoupled. Of course this formulation is equivalent to that developed in Subsection 13.2.3. The latter formulation is apparently more efficient because E_1 is output directly by the eigenvalue-problem solver and meanwhile the amounts of matrix computation to construct the coefficient matrices of the eigenvalue problems in both formulations are about the same.

13.3.3 Anisotropic gratings

In this subsection we continue to assume the grating profile is slanted and the diffraction mounting is conical. Both the incident region and the emergent region are isotropic, but the periodic region is anisotropic. This is the most commonly encountered situation of anisotropic gratings. However, to achieve maximum generality without sacrificing clarity (in fact, to enhance clarity) we assume that the medium anisotropy is in both permittivity and permeability. Allowing anisotropic permeability preserves the formal electromagnetic symmetry of the derived formulas and helps their derivation. Figure 13.5 also depicts the present diffraction problem. The Rayleigh expansions given by (13.62), (13.63), (13.86), and (13.87) are still valid. We only need to find expressions of the total fields in the periodic layer.

For additional readings on the Fourier modal method for one-dimensional periodic gratings made with anisotropic materials the reader may consult references [13.17-21].

13.3.3.1 Fourier factorization of constitutive relations

In an anisotropic medium the two Maxwell equations containing curl operators written in the oblique Cartesian coordinate system of (13.35a) are

$$\xi^{\rho\sigma\tau} \partial_\sigma E_\tau = \mathrm{i} k_0 \sqrt{g}\, \mu^{\rho\sigma} H_\sigma, \tag{13.96a}$$

$$\xi^{\rho\sigma\tau} \partial_\sigma H_\tau = -\mathrm{i} k_0 \sqrt{g}\, \varepsilon^{\rho\sigma} E_\sigma. \tag{13.96b}$$

The permittivity tensor $\varepsilon^{\rho\sigma}$ and permeability tensor $\mu^{\rho\sigma}$ are related to their counterparts $\bar{\varepsilon}^{\rho\sigma}$ and $\bar{\mu}^{\rho\sigma}$ in the normal rectangular Cartesian system by tensor transformation

$$\varepsilon^{\rho\sigma} = \frac{\partial x^\rho}{\partial \bar{x}^{\rho'}} \frac{\partial x^\sigma}{\partial \bar{x}^{\sigma'}} \bar{\varepsilon}^{\rho'\sigma'}, \qquad \mu^{\rho\sigma} = \frac{\partial x^\rho}{\partial \bar{x}^{\rho'}} \frac{\partial x^\sigma}{\partial \bar{x}^{\sigma'}} \bar{\mu}^{\rho'\sigma'}, \tag{13.97}$$

where $\bar{x}^1 = x$, $\bar{x}^2 = y$, and $\bar{x}^3 = z$. Note that the tensor characteristics of $\varepsilon^{\rho\sigma}$ and $\mu^{\rho\sigma}$ come from two sources: the tensor characteristics of $\bar{\varepsilon}^{\rho\sigma}$ and $\bar{\mu}^{\rho\sigma}$ and the coordinate transformation. So, the presence of either one or both results in the same mathematical complexity, although the former source is physical and the latter is mathematical.

In a one-dimensional grating problem $\varepsilon^{\rho\sigma}$ and $\mu^{\rho\sigma}$ depend only on x^1 and their functional dependences on x^1 may be discontinuous. To solve the problem by the Fourier modal method, we need to write $\mathbf{D} = \boldsymbol{\varepsilon} \cdot \mathbf{E} = \varepsilon^{\rho\sigma} E_\sigma$ and $\mathbf{B} = \boldsymbol{\mu} \cdot \mathbf{H} = \mu^{\rho\sigma} H_\sigma$ in Fourier space in a way consistent with the Fourier factorization theory. The first equation in component form can be arranged as

$$D^1 = \varepsilon^{11}\left[E_1 + \left(\frac{\varepsilon^{12}}{\varepsilon^{11}}\right)E_2 + \left(\frac{\varepsilon^{13}}{\varepsilon^{11}}\right)E_3\right], \tag{13.98a}$$

$$D^2 = \left(\frac{\varepsilon^{21}}{\varepsilon^{11}}\right)D^1 + \left(\varepsilon^{22} - \frac{\varepsilon^{21}\varepsilon^{12}}{\varepsilon^{11}}\right)E_2 + \left(\varepsilon^{23} - \frac{\varepsilon^{21}\varepsilon^{13}}{\varepsilon^{11}}\right)E_3, \tag{13.98b}$$

$$D^3 = \left(\frac{\varepsilon^{31}}{\varepsilon^{11}}\right)D^1 + \left(\varepsilon^{32} - \frac{\varepsilon^{31}\varepsilon^{12}}{\varepsilon^{11}}\right)E_2 + \left(\varepsilon^{33} - \frac{\varepsilon^{31}\varepsilon^{13}}{\varepsilon^{11}}\right)E_3. \tag{13.98c}$$

In these equations all products between field components and permittivity-element dependent functions are Type 1 or Type 2 as defined in Subsection 13.2.2.2. So, the Fourier coefficients of vector **D** in terms of those of **E** are

$$D_m^\sigma = (\varepsilon^{\sigma\tau} E_\tau)_m = \sum_n (\hat{\varepsilon}^{\sigma\tau})_{mn} E_{\tau n}, \tag{13.99a}$$

where m and n are Fourier indices, and

$$\hat{\boldsymbol{\varepsilon}} = \begin{pmatrix} \left[\!\left[\frac{1}{\varepsilon^{11}}\right]\!\right]^{-1} & \left[\!\left[\frac{1}{\varepsilon^{11}}\right]\!\right]^{-1}\left[\!\left[\frac{\varepsilon^{12}}{\varepsilon^{11}}\right]\!\right] & \left[\!\left[\frac{1}{\varepsilon^{11}}\right]\!\right]^{-1}\left[\!\left[\frac{\varepsilon^{13}}{\varepsilon^{11}}\right]\!\right] \\ \left[\!\left[\frac{\varepsilon^{21}}{\varepsilon^{11}}\right]\!\right]\left[\!\left[\frac{1}{\varepsilon^{11}}\right]\!\right]^{-1} & \left[\!\left[\frac{\varepsilon^{21}}{\varepsilon^{11}}\right]\!\right]\left[\!\left[\frac{1}{\varepsilon^{11}}\right]\!\right]^{-1}\left[\!\left[\frac{\varepsilon^{12}}{\varepsilon^{11}}\right]\!\right] + \left[\!\left[\varepsilon^{22} - \frac{\varepsilon^{21}\varepsilon^{12}}{\varepsilon^{11}}\right]\!\right] & \left[\!\left[\frac{\varepsilon^{21}}{\varepsilon^{11}}\right]\!\right]\left[\!\left[\frac{1}{\varepsilon^{11}}\right]\!\right]^{-1}\left[\!\left[\frac{\varepsilon^{13}}{\varepsilon^{11}}\right]\!\right] + \left[\!\left[\varepsilon^{23} - \frac{\varepsilon^{31}\varepsilon^{13}}{\varepsilon^{11}}\right]\!\right] \\ \left[\!\left[\frac{\varepsilon^{31}}{\varepsilon^{11}}\right]\!\right]\left[\!\left[\frac{1}{\varepsilon^{11}}\right]\!\right]^{-1} & \left[\!\left[\frac{\varepsilon^{31}}{\varepsilon^{11}}\right]\!\right]\left[\!\left[\frac{1}{\varepsilon^{11}}\right]\!\right]^{-1}\left[\!\left[\frac{\varepsilon^{12}}{\varepsilon^{11}}\right]\!\right] + \left[\!\left[\varepsilon^{32} - \frac{\varepsilon^{31}\varepsilon^{12}}{\varepsilon^{11}}\right]\!\right] & \left[\!\left[\frac{\varepsilon^{31}}{\varepsilon^{11}}\right]\!\right]\left[\!\left[\frac{1}{\varepsilon^{11}}\right]\!\right]^{-1}\left[\!\left[\frac{\varepsilon^{13}}{\varepsilon^{11}}\right]\!\right] + \left[\!\left[\varepsilon^{33} - \frac{\varepsilon^{31}\varepsilon^{13}}{\varepsilon^{11}}\right]\!\right] \end{pmatrix}. \tag{13.100}$$

This expression of permittivity tensor $\vec{\boldsymbol{\varepsilon}}$ in Fourier space is bulky and complicated, but theoretical analysis and numerical tests have shown that it is worth the trouble because it leads to superior numerical performance for grating materials with a large permittivity contrast.

The seemingly complicated expression actually follows a simple construction rule. For any 3×3 matrix **A** with elements $A^{\rho\sigma}$, where ρ, σ = 1, 2, 3 and $A^{\rho\sigma}$ can be a number or a square matrix, provided that $(A^{\tau\tau})^{-1}$ exists for a fixed τ, we define operator $l_\tau^\pm$ by $\mathbf{Z} = l_\tau^\pm(\mathbf{A})$ with

$$Z^{\rho\sigma} = \begin{cases} (A^{\tau\tau})^{-1}, & \rho = \tau, \sigma = \tau; \\ (A^{\tau\tau})^{-1} A^{\tau\sigma}, & \rho = \tau, \sigma \neq \tau; \\ A^{\rho\tau}(A^{\tau\tau})^{-1}, & \rho \neq \tau, \sigma = \tau; \\ A^{\rho\sigma} \pm A^{\rho\tau}(A^{\tau\tau})^{-1} A^{\tau\sigma}, & \rho \neq \tau, \sigma \neq \tau. \end{cases} \tag{13.101}$$

For matrix $Z^{\rho\sigma}(x^1,x^2,x^3)$ we further define F_τ to be an operator such that $\mathbf{C} = F_\tau(\mathbf{Z})$ is a block matrix whose elements $C^{\rho\sigma}$ are Toeplitz matrices generated by the Fourier coefficients of $Z^{\rho\sigma}(x^1,x^2,x^3)$ with respect to variable x^τ. So, if matrix $Z^{\rho\sigma}$ is $p \times p$, then $C^{\rho\sigma}$ is $pm \times pm$, where m is the truncation number in Fourier space. With this apparatus, (13.100) can be written succinctly as

$$\hat{\boldsymbol{\varepsilon}} = l_1^+ F_1 l_1^-(\boldsymbol{\varepsilon}). \tag{13.102a}$$

The efficiency and preciseness of this notation is evident. This will be further demonstrated when we deal with crossed gratings in Section 13.4.

For the magnetic relations we similarly have

$$B_m^{\sigma} = (\mu^{\sigma\tau} H_{\tau})_m = \sum_n (\hat{\mu}^{\sigma\tau})_{mn} H_{\tau n}\,, \tag{13.99b}$$

$$\hat{\boldsymbol{\mu}} = l_1^{+} F_1 l_1^{-}(\boldsymbol{\mu}). \tag{13.102b}$$

13.3.3.2 Construction of the total fields

For Maxwell equations as complex as (13.96), it is advantageous to perform Fourier factorization at the very beginning. In the following we will use E_1, and H_2, etc., to denote column vectors of the Fourier coefficients of $E_1(x^1, x^2, x^3)$ and $H_2(x^1, x^2, x^3)$, respectively. The effects of applying operators ∂_1 and ∂_2 on these functions are to multiply them from the left side by $\mathrm{i}\boldsymbol{\alpha}$ and $\mathrm{i}\beta_0$, where $\boldsymbol{\alpha}$ is a diagonal matrix with elements α_n. Then in Fourier space and in expanded form (13.96) becomes

$$\boldsymbol{\alpha} E_2 - \beta_0 E_1 = k_0^{*}(\hat{\mu}^{31} H_1 + \hat{\mu}^{32} H_2 + \hat{\mu}^{33} H_3), \tag{13.103a}$$

$$\beta_0 E_3 - (\partial_3/\mathrm{i})\, E_2 = k_0^{*}(\hat{\mu}^{11} H_1 + \hat{\mu}^{12} H_2 + \hat{\mu}^{13} H_3), \tag{13.103b}$$

$$(\partial_3/\mathrm{i})\, E_1 - \boldsymbol{\alpha} E_3 = k_0^{*}(\hat{\mu}^{21} H_1 + \hat{\mu}^{22} H_2 + \hat{\mu}^{23} H_3); \tag{13.103c}$$

$$\boldsymbol{\alpha} H_2 - \beta_0 H_1 = -k_0^{*}(\hat{\varepsilon}^{31} E_1 + \hat{\varepsilon}^{32} E_2 + \hat{\varepsilon}^{33} E_3), \tag{13.104a}$$

$$\beta_0 H_3 - (\partial_3/\mathrm{i})\, H_2 = -k_0^{*}(\hat{\varepsilon}^{11} E_1 + \hat{\varepsilon}^{12} E_2 + \hat{\varepsilon}^{13} E_3), \tag{13.104b}$$

$$(\partial_3/\mathrm{i})\, H_1 - \boldsymbol{\alpha} H_3 = -k_0^{*}(\hat{\varepsilon}^{21} E_1 + \hat{\varepsilon}^{22} E_2 + \hat{\varepsilon}^{23} E_3). \tag{13.104c}$$

From (13.103a) and (13.104a), the third field components E_3 and H_3 can be expressed in terms of the first and second components:

$$E_3 = -\frac{1}{k_0^{*}}(\hat{\varepsilon}^{33})^{-1}(\boldsymbol{\alpha} H_2 - \beta_0 H_1) - (\hat{\varepsilon}^{33})^{-1}\hat{\varepsilon}^{31} E_1 - (\hat{\varepsilon}^{33})^{-1}\hat{\varepsilon}^{32} E_2\,. \tag{13.105a}$$

$$H_3 = \frac{1}{k_0^{*}}(\hat{\mu}^{33})^{-1}(\boldsymbol{\alpha} E_2 - \beta_0 E_1) - (\hat{\mu}^{33})^{-1}\hat{\mu}^{31} H_1 - (\hat{\mu}^{33})^{-1}\hat{\mu}^{32} H_2\,. \tag{13.105b}$$

Substituting (13.105) into (13.103) and (13.104) gives

$$(\partial_3/\mathrm{i})\,(E_1, E_2, H_1, H_2)^{\mathrm{T}} = \mathbf{M}\,(E_1, E_2, H_1, H_2)^{\mathrm{T}}\,, \tag{13.106}$$

where the superscript T denotes block matrix transpose,

$$\mathbf{M} = \begin{pmatrix} -\tilde{\mu}^{23}\beta_0 - \boldsymbol{\alpha}\tilde{\varepsilon}^{31} & \tilde{\mu}^{23}\boldsymbol{\alpha} - \boldsymbol{\alpha}\tilde{\varepsilon}^{32} & k_0^{*}\tilde{\mu}^{21} + \frac{1}{k_0^{*}}\boldsymbol{\alpha}\tilde{\varepsilon}^{33}\beta_0 & k_0^{*}\tilde{\mu}^{22} - \frac{1}{k_0^{*}}\boldsymbol{\alpha}\tilde{\varepsilon}^{33}\boldsymbol{\alpha} \\ \tilde{\mu}^{13}\beta_0 - \beta_0\tilde{\varepsilon}^{31} & -\tilde{\mu}^{13}\boldsymbol{\alpha} - \beta_0\tilde{\varepsilon}^{32} & -k_0^{*}\tilde{\mu}^{11} + \frac{1}{k_0^{*}}\beta_0\tilde{\varepsilon}^{33}\beta_0 & -k_0^{*}\tilde{\mu}^{12} - \frac{1}{k_0^{*}}\beta_0\tilde{\varepsilon}^{33}\boldsymbol{\alpha} \\ -k_0^{*}\tilde{\varepsilon}^{21} - \frac{1}{k_0^{*}}\boldsymbol{\alpha}\tilde{\mu}^{33}\beta_0 & -k_0^{*}\tilde{\varepsilon}^{22} + \frac{1}{k_0^{*}}\boldsymbol{\alpha}\tilde{\mu}^{33}\boldsymbol{\alpha} & -\tilde{\varepsilon}^{23}\beta_0 - \boldsymbol{\alpha}\tilde{\mu}^{31} & \tilde{\varepsilon}^{23}\boldsymbol{\alpha} - \boldsymbol{\alpha}\tilde{\mu}^{32} \\ k_0^{*}\tilde{\varepsilon}^{11} - \frac{1}{k_0^{*}}\beta_0\tilde{\mu}^{33}\beta_0 & k_0^{*}\tilde{\varepsilon}^{12} + \frac{1}{k_0^{*}}\beta_0\tilde{\mu}^{33}\boldsymbol{\alpha} & \tilde{\varepsilon}^{13}\beta_0 - \beta_0\tilde{\mu}^{31} & -\tilde{\varepsilon}^{13}\boldsymbol{\alpha} - \beta_0\tilde{\mu}^{32} \end{pmatrix}, \tag{13.107}$$

and

$$\tilde{\boldsymbol{\varepsilon}} = l_3^-(\hat{\boldsymbol{\varepsilon}}) = l_3^- l_1^+ F_1 l_1^-(\boldsymbol{\varepsilon}), \quad \tilde{\boldsymbol{\mu}} = l_3^-(\hat{\boldsymbol{\mu}}) = l_3^- l_1^+ F_1 l_1^-(\boldsymbol{\mu}). \tag{13.108}$$

In writing (13.107) we have left the scalar β_0 where it was dropped down during differentiation relative to other matrices in a product, as if β_0 were a matrix. The reason for doing so will become apparent in Section 13.4. Since **M** does not depend on x^3, the modal function has this dependence $\exp(\mathrm{i}\gamma x^3)$ on x^3 and, after the operator (∂_3/i) is replaced with γ, (13.106) becomes an eigenvalue problem.

If the Fourier-Floquet series representing each field components is truncated from m_1 to $m_2 = N + m_1 - 1$, then **M** is $4N \times 4N$. Partition of the $4N$ eigensolutions follows the same principle as described in Subsection 13.2.3.3, namely, place all eigenvalues with positive and negative imaginary parts in σ^+ and σ^-, respectively, and divide the rest arbitrarily so that σ^+ and σ^- each contains $2N$ eigenvalues. Now the index q for eigensolutions runs from 1 to $2N$. Analogous to (13.51), we have

$$\begin{pmatrix} E_1 \\ E_2 \\ H_1 \\ H_2 \end{pmatrix} = \sum_{m=m_1}^{m_2} \exp(\mathrm{i}\alpha_m x^1 + \mathrm{i}\beta_0 x^2) \sum_{q=1}^{2N} \begin{pmatrix} E_{1mq}^+ & E_{1mq}^- \\ E_{2mq}^+ & E_{2mq}^- \\ H_{1mq}^+ & H_{1mq}^- \\ H_{2mq}^+ & H_{2mq}^- \end{pmatrix} \begin{pmatrix} \exp[\mathrm{i}\gamma_q^+(x^3 - x_0^3)] & 0 \\ 0 & \exp[\mathrm{i}\gamma_q^-(x^3 - x_1^3)] \end{pmatrix} \begin{pmatrix} \tilde{u}_q \\ \tilde{d}_q \end{pmatrix}. \tag{13.109}$$

The eigenvector matrix in (13.109) is the $\mathbf{W}^{(1)}$ matrix in the S-matrix algorithm formulation. Together with the $\mathbf{W}^{(0)}$ and $\mathbf{W}^{(2)}$ matrices given by (13.90) the unknown Rayleigh amplitudes in the homogeneous regions can be solved by using the S-matrix algorithm.

13.3.3.3 Special cases

Equation (13.107) defines the most general eigenvalue problem treated so far in this chapter. By separately or simultaneously setting $\beta_0 = 0$, $\zeta = 0$, and letting $\bar{\varepsilon}^{ij}$ and $\bar{\mu}^{ij}$ to be scalars or to take a special orientation, eigenvalue problems for various special cases can be obtained. For example, if $\beta_0 = 0$, $\bar{\varepsilon}^{12} = \bar{\varepsilon}^{21} = \bar{\varepsilon}^{23} = \bar{\varepsilon}^{32} = 0$, and $\bar{\mu}^{12} = \bar{\mu}^{21} = \bar{\mu}^{23} = \bar{\mu}^{32} = 0$, then regardless of slant angle ζ only elements on the two diagonal lines of **M** are nonzero. So, the eigenvalue problem breaks up into two $2N \times 2N$ problems and the field components E_1 and H_2 are decoupled from E_2 and H_1. However, for slanted isotropic gratings in conical mounting the eigenvalue problem does not break up into two $2N \times 2N$ problems; the $2N \times 2N$ eigenvalue problems of Subsection 13.3.2.2 does not follow from the current formulation.

13.4 Crossed anisotropic gratings

For additional readings on the Fourier modal method for crossed gratings the reader may consult Chapter 7 of this book and references [13.22-28].

13.4.1 Description of the problem of crossed anisotropic gratings

A crossed grating can be defined as a planar layer of finite thickness whose optical properties vary periodically along two noncollinear directions. Other names are two-dimensional gratings and bigratings, but these names are sometimes used to mean other things. It is self evident that once a two dimensional structure is periodic in two noncollinear directions, it is periodic in countably infinite directions. We choose two directions that make an angle closest to $\pi/2$ as the principal periodic directions, or simply the periodic directions, of the grating, and define the smallest periods along the two directions as the periods of the grating. In most theoretical treatments of crossed gratings the two periodic directions are assumed to be mutually orthogonal, and many crossed gratings in applications indeed have this property. How-

ever, exceptions are common, so we do not make this assumption. The cost for accommodating nonorthogonality is not much, especially in dealing with anisotropic gratings.

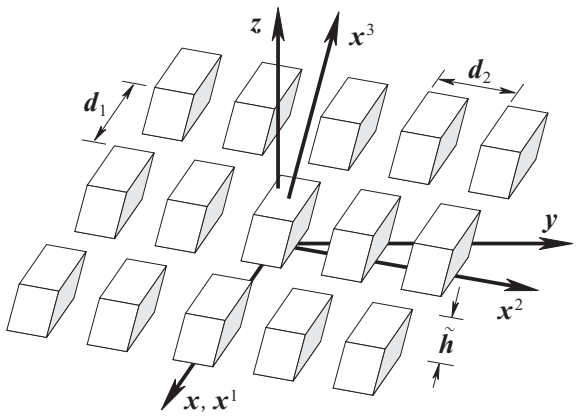

Fig. 13.6. Definition and notation of a crossed grating problem. All surfaces of the rhombs are parallel to a coordinate surface of the skew Cartesian coordinate system $Ox^1x^2x^3$ defined in Fig. 13.7.

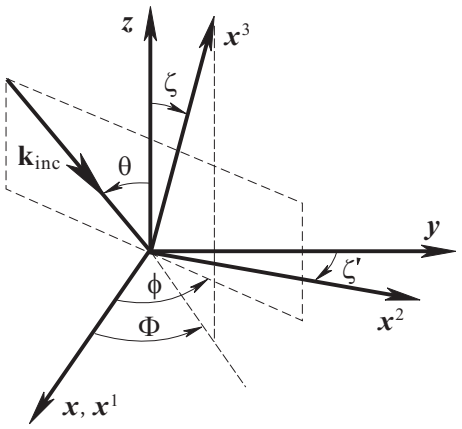

Fig. 13.7. Definition of the skew Cartesian coordinate system Ox1x2x3 relative to the rectangular Cartesian coordinate system Oxyz and definition of the angles of incidence. The axis x1 coincides with the axis x, and the three axes x1, x2, and y are all in the grating plane.

We consider the most general crossed gratings made with materials of anisotropic permittivity and permeability, but limit the grating profile to those that can be treated by the Fourier modal method the most efficiently, i.e., all grating surfaces are assumed to be parallel to one of the coordinate planes of a skew Cartesian coordinate system $Ox^1x^2x^3$. Figure 13.6 depicts such a crossed grating. The x^1 and x^2 axes are along the two periodic directions, so the x^1x^2 plane is the grating plane. The two grating periods are d_1 and d_2, and the pillar height $\tilde{h}$ is measured along the x^3 direction. The three axes are in general not mutually orthogonal and their relationship with respect to the conventional rectangular Cartesian coordinate system is defined in Fig. 13.7. The x axis coincides with the x^1 axis, and the xy plane coincides with the x^1x^2 plane. ζ' is the angle between the x^2 and y axes, ζ is the angle between the x^3 and z axes, and Φ is the angle between the x axis and the projection of the x^3 axis on the xy plane. Therefore, the two coordinate systems are related by

$$x = x^1 + x^2 \sin\zeta' + x^3 \sin\zeta \cos\Phi, \quad y = x^2 \cos\zeta' + x^3 \sin\zeta \sin\Phi, \quad z = x^3 \cos\zeta. \tag{13.110}$$

The covariant and contravariant basis vectors associated with this coordinate system are

$$\mathbf{b}_1 = \hat{\mathbf{x}}, \quad \mathbf{b}_2 = \hat{\mathbf{x}} \sin\zeta' + \hat{\mathbf{y}} \cos\zeta', \quad \mathbf{b}_3 = \hat{\mathbf{x}} \sin\zeta \cos\Phi + \hat{\mathbf{y}} \sin\zeta \sin\Phi + \hat{\mathbf{z}} \cos\zeta, \tag{13.111}$$

$$\begin{aligned} \mathbf{b}^1 &= \hat{\mathbf{x}} - \hat{\mathbf{y}} \tan\zeta' - \hat{\mathbf{z}} \tan\zeta \sec\zeta' \cos(\Phi + \zeta'), \\ \mathbf{b}^2 &= \hat{\mathbf{y}} \sec\zeta' - \hat{\mathbf{z}} \tan\zeta \sec\zeta' \sin\Phi, \\ \mathbf{b}^3 &= \hat{\mathbf{z}} \sec\zeta. \end{aligned} \tag{13.112}$$

respectively. The metric tensors $g^{\rho\sigma}$ and $g_{\rho\sigma}$ can be calculated from the basis vectors using formula (13.39). The permittivity tensor $\varepsilon^{\rho\sigma}$ and permeability tensor $\mu^{\rho\sigma}$ in this coordinate system are related to their counterparts $\overline{\varepsilon}^{\rho\sigma}$ and $\overline{\mu}^{\rho\sigma}$ in the rectangular Cartesian system in the same way as in (13.97).

For specification of incident angles and state of polarization of the incident plane wave we use the rectangular Cartesian coordinate system as usual. The incident polar angle θ and azimuth angle ϕ are defined in Fig. 13.7. The method of defining state of polarization is the same as in Subsection 13.3.1. The wave vector of the incident plane wave in the skew coordinate system is

$$\mathbf{k}_{\text{inc}} = \mathbf{b}^1 \alpha_0 + \mathbf{b}^2 \beta_0 + \mathbf{b}^3 \gamma_{00}^{(2)-}, \tag{13.113}$$

where

$$\begin{aligned} \alpha_0 &= k^{(2)} \sin\theta \cos\phi, \\ \beta_0 &= k^{(2)} \sin\theta \sin(\phi + \zeta'), \\ \gamma_{00}^{(2)-} &= k^{(2)} [\sin\zeta \sin\theta \cos(\Phi - \phi) - \cos\theta \cos\zeta]. \end{aligned} \tag{13.114}$$

The notation for the last covariant component will become apparent shortly.

13.4.2 Rayleigh expansions in skew three-dimensional coordinates

The electric field components in the two semi-infinite regions can be written in Rayleigh expansions:

$$\begin{aligned} E_\sigma^{(2)}(x^1, x^2, x^3) &= I_\sigma \exp[\mathrm{i}(\alpha_0 x^1 + \beta_0 x^2 + \gamma_{00}^{(2)-} x^3)] + \\ &\quad + \sum_{m,n} R_{\sigma mn} \exp[\mathrm{i}(\alpha_m x^1 + \beta_n x^2 + \gamma_{mn}^{(2)+} x^3)], \qquad x^3 \ge \tilde{h}; \end{aligned} \tag{13.115a}$$

$$E_\sigma^{(0)}(x^1, x^2, x^3) = \sum_{m,n} T_{\sigma mn} \exp[\mathrm{i}(\alpha_m x^1 + \beta_n x^2 + \gamma_{mn}^{(0)-} x^3)], \qquad x^3 \le 0. \tag{13.115b}$$

where σ = 1, 2, 3, and I_σ, R_σ, and T_σ represent the incident, reflected, and transmitted electric field amplitudes, respectively. In the arguments of the exponential functions,

$$\alpha_m = \alpha_0 + m K_1, \qquad K_1 = 2\pi / d_1, \tag{13.116a}$$

$$\beta_n = \beta_0 + n K_2, \qquad K_2 = 2\pi / d_2, \tag{13.116b}$$

$$\gamma_{mn}^{(p)\pm} = [\pm k_{mn}^{3(p)} - (g^{31}\alpha_m + g^{32}\beta_n)] / g^{33}, \qquad p = 0, 2, \tag{13.117}$$

$$k_{mn}^{3(p)} = [g^{33}(k^{(p)2} - \alpha_m^2 g^{11} - 2\alpha_m \beta_n g^{12} - \beta_n^2 g^{22}) + (g^{31}\alpha_m + g^{32}\beta_n)^2]^{1/2}. \quad p = 0, 2. \tag{13.118}$$

From (13.115) we see that for a crossed grating it takes two indices to label a diffraction order. α_m, β_n, and $\gamma_{mn}^{(p)\pm}$ are the three covariant components and $k_{mn}^{3(p)}$ is the third contravariant component of the wave vector of the (m,n)th diffraction order, respectively. The sign of $k_{mn}^{3(p)}$ should be chosen so that

$$\mathrm{Re}[k_{mn}^{3(p)}] + \mathrm{Im}[k_{mn}^{3(p)}] > 0. \qquad p = 0, 2. \tag{13.119}$$

In this way the sum containing $\gamma_{mn}^{(p)+}$ in (13.115a) and that containing $\gamma_{mn}^{(p)-}$ in (115b) properly represent reflected and transmitted waves, respectively. The diffraction orders with a real $k_{mn}^{3(p)}$ are propagating and the rest with a nonzero imaginary part are evanescent.

The (m,n)th-order diffracted wave vector can be written as

$$\mathbf{k}_{mn}^{(p)} = \alpha_m \mathbf{b}^1 + \beta_n \mathbf{b}^2 + \gamma_{mn}^{(p)\pm} \mathbf{b}^3, \tag{13.120}$$

where the upper and lower signs are chosen for p = 2 and 0, respectively. The perpendicular projection of $\mathbf{k}_{mn}^{(p)}$ onto the grating plane, denoted by $\mathbf{k}_{mn}^{\perp}$, is the same in both regions:

$$\mathbf{k}_{mn}^{\perp} = \alpha_m \mathbf{b}_{\perp}^1 + \beta_n \mathbf{b}_{\perp}^2, \qquad \mathbf{b}_{\perp}^1 = \hat{\mathbf{x}} - \hat{\mathbf{y}} \tan\zeta', \qquad \mathbf{b}_{\perp}^2 = \hat{\mathbf{y}} \sec\zeta'. \tag{13.121}$$

$\mathbf{k}_{mn}^{\perp}$ can be written in another form

$$\mathbf{k}_{mn}^{\perp} = \mathbf{k}_{00}^{\perp} + \mathbf{K}_{mn}, \qquad \mathbf{K}_{mn} = m K_1 \mathbf{b}_{\perp}^1 + n K_2 \mathbf{b}_{\perp}^2. \tag{13.122}$$

Here $\mathbf{K}_{mn}$ defines the reciprocal space lattice of the crossed grating. It is reciprocal to the real space lattice

$$\mathbf{G}_{mn} = m d_1 \mathbf{b}_1 + n d_2 \mathbf{b}_2. \tag{13.123}$$

Figure 13.8 depicts an example of real space lattice and its reciprocal space lattice. Note that the periodic directions of the two lattices of differing indices are mutually orthogonal, but the periodic directions of the same indices are not parallel to each other, unless the lattices are rectangular. It is important to realize that $\mathbf{K}_{mn}$ together with $\mathbf{k}_{00}^{\perp}$, not $\mathbf{G}_{mn}$, gives the direction of the (m,n)th diffraction order in the grating plane.

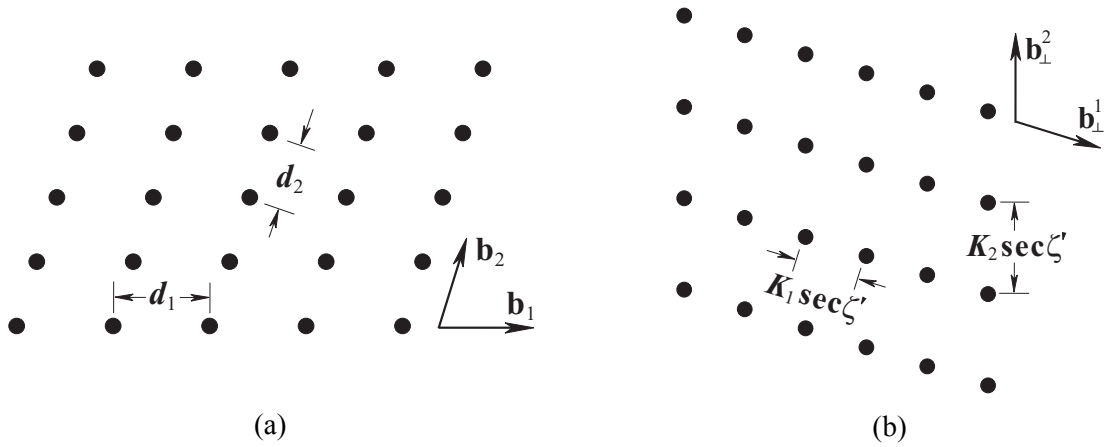

Fig. 13.8. Real space lattice (a) *and reciprocal space lattice* (b) of *a crossed grating.*

Among the six electromagnetic field components of a plane wave in a homogeneous medium, we choose E_1 and E_2 as the two independent ones. This is possible, unless $k_{mn}^{3(p)} = 0$ for some integers m and n. Since $k_{mn}^{3(p)}$ is the component of a diffracted order perpendicular to the grating plane, $k_{mn}^{3(p)} = 0$ means the diffracted order is propagating parallel to this plane, i.e., Rayleigh anomaly occurs. This situation can be avoided by slightly changing the incident angle, or wavelength, or grating period(s). The magnetic field components can be obtained from Maxwell equations. After this is done, the column vector of Fourier coefficients of the four total electromagnetic field components parallel to the grating plane in the two homogeneous regions are given by

$$\begin{pmatrix} E_{1mn}^{(p)} \\ E_{2mn}^{(p)} \\ H_{1mn}^{(p)} \\ H_{2mn}^{(p)} \end{pmatrix} = \begin{pmatrix} 1 & 0 & 1 & 0 \\ 0 & 1 & 0 & 1 \\ -C_{mn}^{(p)} & -A_{mn}^{(p)} & C_{mn}^{(p)} & A_{mn}^{(p)} \\ B_{mn}^{(p)} & C_{mn}^{(p)} & -B_{mn}^{(p)} & -C_{mn}^{(p)} \end{pmatrix} \begin{pmatrix} D_{mn}^{(p)+} & 0 & 0 & 0 \\ 0 & D_{mn}^{(p)+} & 0 & 0 \\ 0 & 0 & D_{mn}^{(p)-} & 0 \\ 0 & 0 & 0 & D_{mn}^{(p)-} \end{pmatrix} \begin{pmatrix} \tilde{u}_{1mn}^{(p)} \\ \tilde{u}_{2mn}^{(p)} \\ \tilde{d}_{1mn}^{(p)} \\ \tilde{d}_{2mn}^{(p)} \end{pmatrix}, \tag{13.124}$$

where $p = 0, 2$, $A_{mn}^{(p)}$, $B_{mn}^{(p)}$, $C_{mn}^{(p)}$, and $D_{mn}^{(p)\pm}$ are diagonal matrices with elements

$$A_{mn}^{(p)} = \frac{k^{(p)2} - \alpha_m^2}{k_0^{**} \mu^{(p)} k_{mn}^{3(p)}}, \quad B_{mn}^{(l)} = \frac{k^{(p)2} - \beta_n^2}{k_0^{**} \mu^{(p)} k_{mn}^{3(p)}}, \quad C_{mn}^{(p)} = \frac{\alpha_m \beta_n - \sin\zeta' k^{(p)2}}{k_0^{**} \mu^{(p)} k_{mn}^{3(p)}}, \tag{13.125a}$$

$$D_{mn}^{(p)+} = \exp[\mathrm{i}\gamma_{mn}^{(p)+}(x^3 - x_{p-1}^3)], \quad D_{mn}^{(p)-} = \exp[\mathrm{i}\gamma_{mn}^{(p)-}(x^3 - x_p^3)], \tag{13.125b}$$

$k_0^{**} = k_0 \cos\zeta \cos\zeta'$, $\mu^{(p)}$ is the scalar magnetic permeability of region p, $p = 0, 2$, $\tilde{u}_{\sigma mn}^{(2)} = R_{\sigma mn} \exp(\mathrm{i}\gamma_{mn}^{(2)+} x_1^3)$, $\tilde{u}_{\sigma mn}^{(0)} = 0$, $\tilde{d}_{\sigma mn}^{(2)} = I_\sigma \delta_{m0} \delta_{n0} \exp(\mathrm{i}\gamma_{00}^{(2)-} x_2^3)$, and $\tilde{d}_{\sigma mn}^{(0)} = T_{\sigma mn} \exp(\mathrm{i}\gamma_{mn}^{(0)-} x_0^3)$. The first and second square matrices in (13.124) are the $\mathrm{W}^{(p)}$ and $\phi^{(p)}$ matrices in the S matrix propagation algorithm. The diffraction efficiencies are given by

$$\eta_{mn}^{(2)} = A_{mn}^{(2)} |R_{2mn}|^2 + B_{mn}^{(2)} |R_{1mn}|^2 + C_{mn}^{(2)} (R_{1mn} \overline{R_{2mn}} + R_{2mn} \overline{R_{1mn}}), \tag{13.126a}$$

$$\eta_{mn}^{(0)} = A_{mn}^{(0)} |T_{2mn}|^2 + B_{mn}^{(0)} |T_{1mn}|^2 + C_{mn}^{(0)} (T_{1mn} \overline{T_{2mn}} + T_{2mn} \overline{T_{1mn}}), \tag{13.126b}$$

provided that

$$A_{00}^{(2)} |I_2|^2 + B_{00}^{(2)} |I_1|^2 + C_{00}^{(2)} (I_1 \overline{I_2} + I_2 \overline{I_1}) = 1, \tag{13.127}$$

and (m,n) makes $k_{mn}^{3(p)}$ real, where the bar means complex conjugation.

13.4.3 Fourier factorization of the constitutive relations

To apply the Fourier modal method to crossed anisotropic gratings we need to first write $\varepsilon^{\rho\sigma} E_\sigma$ and $\mu^{\rho\sigma} H_\sigma$ in two-dimensional Fourier space. Now $\varepsilon^{\rho\sigma}$ and $\mu^{\rho\sigma}$ are independent of x^3. Again, it is sufficient to work with $\varepsilon^{\rho\sigma} E_\sigma$ only. The Fourier transforms along x^1 and x^2 are to be done one at a time. Suppose we do it along x^1 first, then the analysis that we have carried out in Subsection 13.3.3.1 can be repeated here without change, because E_2, E_3, and D^1 are still continuous with respect to variable x^1, independent of parameter x^2. Therefore, from (13.99),

$$D_m^\rho(x^2) = (\varepsilon^{\rho\sigma} E_\sigma)_m(x^2) = \sum_n (\hat{\varepsilon}_1^{\rho\sigma})_{mn} E_{\sigma n}(x^2), \tag{13.128}$$

where we have used the subscript 1 in $\hat{\varepsilon}_1^{ij}$ to indicate that the Fourier transform is along x^1. Equation (13.128) is yet to be Fourier transformed along x^2, which can be done in a similar way. We write the equation as follows, dropping the x^2 dependence for simplicity,

$$D_m^1 = \sum_n \left\{ [\hat{\varepsilon}_1^{11} - \hat{\varepsilon}_1^{12}(\hat{\varepsilon}_1^{22})^{-1}\hat{\varepsilon}_1^{21}]_{mn} E_{1n} + [\hat{\varepsilon}_1^{12}(\hat{\varepsilon}_1^{22})^{-1}]_{mn} D_n^2 + [\hat{\varepsilon}_1^{13} - \hat{\varepsilon}_1^{12}(\hat{\varepsilon}_1^{22})^{-1}\hat{\varepsilon}_1^{23}]_{mn} E_{3n} \right\}, \tag{13.129a}$$

$$E_{2m} = \sum_n \left\{ (\hat{\varepsilon}_1^{22})_{mn}^{-1} D_n^2 - [(\hat{\varepsilon}_1^{22})^{-1}\hat{\varepsilon}_1^{21}]_{mn} E_{1n} - [(\hat{\varepsilon}_1^{22})^{-1}\hat{\varepsilon}_1^{23}]_{mn} E_{3n} \right\}, \tag{13.129b}$$

$$D_m^3 = \sum_n \left\{ [\hat{\varepsilon}_1^{31} - \hat{\varepsilon}_1^{32}(\hat{\varepsilon}_1^{22})^{-1}\hat{\varepsilon}_1^{21}]_{mn} E_{1n} + [\hat{\varepsilon}_1^{32}(\hat{\varepsilon}_1^{22})^{-1}]_{mn} D_n^2 + [\hat{\varepsilon}_1^{33} - \hat{\varepsilon}_1^{32}(\hat{\varepsilon}_1^{22})^{-1}\hat{\varepsilon}_1^{23}]_{mn} E_{3n} \right\}, \tag{13.129c}$$

On the right-hand sides of (13.129) every one of the Fourier coefficient E_{1n}, E_{3n}, and D_n^2 is a continuous function of x^2 (for a proof, see [13.25]); therefore, Laurent's rule can be applied to each scalar product. This gives the result

$$D_{mn}^{\rho} = (\varepsilon^{\rho\sigma} E_{\sigma})_{mn} = \sum_{i,j} (\hat{\varepsilon}_{12}^{\rho\sigma})_{mn,ij} E_{\sigma ij}, \tag{13.130}$$

where

$$\hat{\boldsymbol{\varepsilon}}_{12} = l_2^+ F_2 l_2^- (\hat{\boldsymbol{\varepsilon}}_1) = l_2^+ F_2 l_2^- \, l_1^+ F_1 l_1^- (\boldsymbol{\varepsilon}), \tag{13.131}$$

and we have used the second subscript in $\hat{\varepsilon}_{12}^{\rho\sigma}$ to indicate that the second-time Fourier transform is along x^2.

Unlike the one-dimensional Fourier factorization of $\varepsilon^{\rho\sigma} E_{\sigma}$ where the result is unique, in two-dimensional Fourier factorization the result is not unique. In the above, we could have reversed the order of Fourier transforms, i.e., first along x^2 then along x^1. This would lead to

$$\hat{\boldsymbol{\varepsilon}}_{21} = l_1^+ F_1 l_1^- (\hat{\boldsymbol{\varepsilon}}_2) = l_1^+ F_1 l_1^- \, l_2^+ F_2 l_2^- (\boldsymbol{\varepsilon}), \tag{13.132}$$

which is an equally acceptable expression. In fact, there are a multitude of choices. For example, we can use $\hat{\varepsilon}_{12}^{\rho\sigma}$ for some ρσ combinations and $\hat{\varepsilon}_{21}^{\rho\sigma}$ for the rest, or simply take average of $\hat{\varepsilon}_{12}^{\rho\sigma}$ and $\hat{\varepsilon}_{21}^{\rho\sigma}$ for all ρ and σ. Presumably all choices lead to the same numerical result in the limit of infinite un-truncated Fourier matrices. In finite truncated Fourier space they are slightly different. In most practical applications the differences are unimportant when the numerical results have converged, but under some very special circumstances where the incident plane wave condition, the grating medium anisotropy, and the grating profile altogether support certain symmetry, a choice compatible with the symmetry is obviously preferred. An example of such a case can be found in [13.7]. Ignoring the slight differences, we will drop the subscripts and use $\hat{\varepsilon}^{\rho\sigma}$ to denote the two-dimensional Fourier representation of $\boldsymbol{\varepsilon}$ in what follows.

13.4.4 Fields in the two-dimensionally periodic anisotropic region

Once the Fourier representations of the constitutive relations are obtained, the derivation of the modal fields and the total fields is straight-forward. A covariant component of any modal field vector takes this form

$$F_{\sigma}(x^1, x^2, x^3) = \exp(\mathrm{i}\gamma x^3) \sum_{m,n} \exp(\mathrm{i}\alpha_m x^1 + \mathrm{i}\beta_n x^2) F_{\sigma mn}, \tag{13.133}$$

where F stands for E or H, and σ = 1, 2, 3. After examining the derivation in Subsection 13.3.3.2 the reader can see that almost all results there can be copied here. In particular, (13.103) through (13.107) are valid for crossed anisotropic gratings, provided that k_0^* is re-

placed by k_0^{**}, the scalar β_0 is replaced by diagonal matrix $\boldsymbol{\beta}$ whose elements are $\delta_{mi}\delta_{nj}\beta_n$, and $\boldsymbol{\alpha}$ is understood as $\delta_{mi}\delta_{nj}\alpha_m$. For the sake of saving space, we will not repeat all equations here, except to give the matrix of the eigenvalue problem and the expression of the total fields:

$$\mathbf{M}=\begin{pmatrix} -\tilde{\mu}^{23}\boldsymbol{\beta}-\boldsymbol{\alpha}\tilde{\varepsilon}^{31} & \tilde{\mu}^{23}\boldsymbol{\alpha}-\boldsymbol{\alpha}\tilde{\varepsilon}^{32} & k_0^{**}\tilde{\mu}^{21}+\dfrac{1}{k_0^{**}}\boldsymbol{\alpha}\tilde{\varepsilon}^{33}\boldsymbol{\beta} & k_0^{**}\tilde{\mu}^{22}-\dfrac{1}{k_0^{**}}\boldsymbol{\alpha}\tilde{\varepsilon}^{33}\boldsymbol{\alpha} \\ \tilde{\mu}^{13}\boldsymbol{\beta}-\boldsymbol{\beta}\tilde{\varepsilon}^{31} & -\tilde{\mu}^{13}\boldsymbol{\alpha}-\boldsymbol{\beta}\tilde{\varepsilon}^{32} & -k_0^{**}\tilde{\mu}^{11}+\dfrac{1}{k_0^{**}}\boldsymbol{\beta}\tilde{\varepsilon}^{33}\boldsymbol{\beta} & -k_0^{**}\tilde{\mu}^{12}-\dfrac{1}{k_0^{**}}\boldsymbol{\beta}\tilde{\varepsilon}^{33}\boldsymbol{\alpha} \\ -k_0^{**}\tilde{\varepsilon}^{21}-\dfrac{1}{k_0^{**}}\boldsymbol{\alpha}\tilde{\mu}^{33}\boldsymbol{\beta} & -k_0^{**}\tilde{\varepsilon}^{22}+\dfrac{1}{k_0^{**}}\boldsymbol{\alpha}\tilde{\mu}^{33}\boldsymbol{\alpha} & -\tilde{\varepsilon}^{23}\boldsymbol{\beta}-\boldsymbol{\alpha}\tilde{\mu}^{31} & \tilde{\varepsilon}^{23}\boldsymbol{\alpha}-\boldsymbol{\alpha}\tilde{\mu}^{32} \\ k_0^{**}\tilde{\varepsilon}^{11}-\dfrac{1}{k_0^{**}}\boldsymbol{\beta}\tilde{\mu}^{33}\boldsymbol{\beta} & k_0^{**}\tilde{\varepsilon}^{12}+\dfrac{1}{k_0^{**}}\boldsymbol{\beta}\tilde{\mu}^{33}\boldsymbol{\alpha} & \tilde{\varepsilon}^{13}\boldsymbol{\beta}-\boldsymbol{\beta}\tilde{\mu}^{31} & -\tilde{\varepsilon}^{13}\boldsymbol{\alpha}-\boldsymbol{\beta}\tilde{\mu}^{32} \end{pmatrix}, \quad (13.134)$$

$$\begin{pmatrix} E_1 \\ E_2 \\ H_1 \\ H_2 \end{pmatrix}=\sum_{m,n=m_1}^{m_2}\exp(\mathrm{i}\alpha_m x^1+\mathrm{i}\beta_n x^2)\sum_{q=1}^{2N^2}\begin{pmatrix} E^+_{1mnq} & E^-_{1mnq} \\ E^+_{2mnq} & E^-_{2mnq} \\ H^+_{1mnq} & H^-_{1mnq} \\ H^+_{2mnq} & H^-_{2mnq} \end{pmatrix}\begin{pmatrix} \exp[\mathrm{i}\gamma_q^+(x^3-x_0^3)] & 0 \\ 0 & \exp[\mathrm{i}\gamma_q^-(x^3-x_1^3)] \end{pmatrix}\begin{pmatrix} \tilde{u}_q \\ \tilde{d}_q \end{pmatrix}. \quad (13.135)$$

In (13.134) $\tilde{\boldsymbol{\varepsilon}}=l_3^-(\hat{\boldsymbol{\varepsilon}})$ and $\tilde{\boldsymbol{\mu}}=l_3^-(\hat{\boldsymbol{\mu}})$, and in (13.135) we have assumed that the Fourier space truncation in both x^1 and x^2 directions are from m_1 to $m_2 = N + m_1 - 1$. The eigenvalue partition follows the same principle as explained previously. The eigenvector matrix in (13.135) gives the $\mathbf{W}^{(1)}$ matrix needed to carry out the S-matrix propagation algorithm.

13.5 Staircase approximation and S-matrix algorithm

In this chapter by assuming invariance of medium permittivity and permeability of the grating layer in an out-of-plane direction, the z or x^3 direction, we are able to turn the problem of solving Maxwell equations into that of finding solutions of an eigenvalue problem. The Fourier modal method is the most suitable for this type of grating structures. In particular, its degree of difficulty in numerical solution is independent on groove depth or pillar height. However, the assumption also restricts the applicability of the Fourier modal method because the structural invariance is not always available.

13.5.1 Staircase approximation

A common method to extend the Fourier modal method to grating structures varying in the x^3-direction within the grating layer is to apply the staircase approximation. A grating of arbitrary x^3-direction variation is sliced into many layers parallel to the grating plane and in each layer the medium boundary is locally replaced by an x^3-invariant boundary. Then within each modified layer the Fourier modal method is applicable. The total fields in a modified layer are connected to those of neighboring layers by electromagnetic boundary conditions at the layer interfaces, and ultimately to the two semi-infinite homogeneous regions. In this way solution to the original grating problem is "approximated" by solution to the modified grating problem.

From an intuitive and naïve point of view the staircase approximation seems reasonable. As the number of layers tends to infinity and the maximum layer thickness tends to zero, the modified structure tends the original one, if the observation is made on a fixed length scale. This idea of approximation is similar to that used in elementary calculus to calculate the area

of an arbitrary shape by integrating rectangular infinitesimal area elements dxdy. However, the problem here is physical, not mathematical. Ample numerical experiments have shown that, in case of one-dimensionally periodic gratings, the approximation works well for TE polarization, but not well for TM polarization especially for highly conducting metallic gratings. The reason is electromagnetic. At the sharp edge of a wedge formed by nonmagnetic media of different permittivities, the electric field component parallel to the edge direction is finite but that transverse to the edge direction, if nonzero, is infinite [13.29]. In staircase approximation many edges are artificially created. In TE polarization the electric field remains finite everywhere, so no severe numerical problem is introduced. In TM polarization, the electric field that should be finite near the smooth grating profile becomes infinitely large at the edges of the staircase boundary. In other word, the near field is altered completely. Therefore, the numerical convergence and computation accuracy of far-field properties, such as diffraction efficiency, is severely affected. For one-dimensional gratings in conical mounting and crossed gratings under any incidence condition, electric field components transverse to the sharp edges are unavoidable when staircase approximation is used.

The artificially introduced adverse effect of staircase approximation and its cause were known for a long time, but the first detailed study appeared much later [13.30]. If the approximation were used to study properties of a periodic structure of negative permittivity free of sharp edges, something much worse can happen. For certain combination of negative permittivity and wedge angle no numerical method converges to date [13.31-33].

From computation efficiency point of view staircase approximation is also inadvisable. The computation time required by the approximation is roughly proportional to the number of layers. The more layers are used, the more accurate the numerical results are obtained, but also the more computation time is needed. In general, when a grating of non-staircase profile is encountered, it is advisable to use a method that does not rely on staircase approximation, such as the integral method described in Chapter 4, or the differential method in Chapter 7, or the C method in Chapter 8.

The advantage of staircase approximation, if it works, is that it is simple to implement algorithmically. So, one has to make a tradeoff between programming complexity and computation efficiency. The best way to implement the staircase approximation is to use the S-matrix propagation algorithm.

13.5.2 S-matrix algorithm

Suppose the space is divided into $P + 1$ layers in the direction normal to the grating plane, where $P \geq 1$. Layer 0 is the semi-infinite substrate and layer $P + 1$ is the semi-infinite cover. Layers 1 through layer P are the staircase approximation layers. We assume medium p is between $x^3 = x^3_{p-1}$ and $x^3 = x^3_p$ and has thickness $\tilde{h}_p = x^3_p - x^3_{p-1}$. As demonstrated repeatedly in this chapter the Fourier coefficients of the vector components of the total tangential fields can be written in a standard form:

$$\mathscr{F}^{(p)}(x^3) = (W^{(p)+},\, W^{(p)-}) \begin{pmatrix} \exp[\mathrm{i}\gamma^{(p)+}(x^3 - x^3_{p-1})] & 0 \\ 0 & \exp[\mathrm{i}\gamma^{(p)-}(x^3 - x^3_p)] \end{pmatrix} \begin{pmatrix} \tilde{u}^{(p)} \\ \tilde{d}^{(p)} \end{pmatrix}, \quad (13.136)$$

with

$$\tilde{u}^{(p)}_q = u^{(p)}_q \exp(\mathrm{i}\gamma^{(p)+}_q x^3_{p-1}), \qquad \tilde{d}^{(p)}_q = d^{(p)}_q \exp(\mathrm{i}\gamma^{(p)-}_q x^3_p), \quad (13.137)$$

where $W^{(p)+}$ and $W^{(p)-}$ are 2×1 block matrices and for simplicity we have omitted the subscripts for eigenvalues and modal amplitudes. Matching boundary conditions at $x^3 = x^3_p$ gives $\mathscr{F}^{(p)}(x^3_p - 0) = \mathscr{F}^{(p+1)}(x^3_p + 0)$, i.e.,

$$(W^{(p+1)+},\ W^{(p+1)-})\begin{pmatrix}1 & 0\\ 0 & \phi_-^{(p+1)-1}\end{pmatrix}\begin{pmatrix}\tilde{u}^{(p+1)}\\ \tilde{d}^{(p+1)}\end{pmatrix}=(W^{(p)+},\ W^{(p)-})\begin{pmatrix}\phi_+^{(p)} & 0\\ 0 & 1\end{pmatrix}\begin{pmatrix}\tilde{u}^{(p)}\\ \tilde{d}^{(p)}\end{pmatrix}, \tag{13.138}$$

where

$$\phi_-^{(p)-1}=\exp(-\mathrm{i}\gamma^{(p)-}\tilde{h}_p),\qquad \phi_+^{(p)}=\exp(\mathrm{i}\gamma^{(p)+}\tilde{h}_p). \tag{13.139}$$

In the S-matrix algorithm we seek a set of matrices $S^{(p)}$ that links the inputs and outputs of the layer assemble 0 through p, such that

$$\begin{pmatrix}\tilde{u}^{(p)}\\ \tilde{d}^{(0)}\end{pmatrix}=S^{(p-1)}\begin{pmatrix}\tilde{u}^{(0)}\\ \tilde{d}^{(p)}\end{pmatrix}=\begin{pmatrix}T_{\mathrm{uu}}^{(p-1)} & R_{\mathrm{ud}}^{(p-1)}\\ R_{\mathrm{du}}^{(p-1)} & T_{\mathrm{dd}}^{(p-1)}\end{pmatrix}\begin{pmatrix}\tilde{u}^{(0)}\\ \tilde{d}^{(p)}\end{pmatrix}. \tag{13.140}$$

From (13.138) and (13.140) we obtain a set of recursion formulas for getting $S^{(p)}$ from $S^{(p-1)}$ and the **W** matrices directly:

$$T_{\mathrm{uu}}^{(p)}=(\mathbf{Z}^{-1}X_1)_1, \tag{13.141a}$$

$$R_{\mathrm{ud}}^{(p)}=(\mathbf{Z}^{-1}X_2)_1, \tag{13.141b}$$

$$R_{\mathrm{du}}^{(p)}=R_{\mathrm{du}}^{(p-1)}+T_{\mathrm{dd}}^{(p-1)}(\mathbf{Z}^{-1}X_1)_2, \tag{13.141c}$$

$$T_{\mathrm{dd}}^{(p)}=T_{\mathrm{dd}}^{(p-1)}(\mathbf{Z}^{-1}X_2)_2, \tag{13.141d}$$

where

$$\begin{aligned}\mathbf{Z}&=(W^{(p+1)+},\ -W^{(p)+}\phi_+^{(p)}R_{\mathrm{ud}}^{(p-1)}-W^{(p)-}),\\ X_1&=W^{(p)+}\phi_+^{(p)}T_{\mathrm{uu}}^{(p-1)},\qquad X_2=-W^{(p+1)-}\phi_-^{(p+1)-1}.\end{aligned} \tag{13.142}$$

In (13.141) the subscripts 1 and 2 attached to the parentheses refer to the upper and lower block of the matrix enclosed. The S-matrix recursion can be initialized with $S^{(-1)}$ being an identity matrix, and continued until $S^{(P)}$ is obtained, which links the Rayleigh amplitudes in the two semi-infinite regions. For most applications $\tilde{u}^{(0)}=0$, so only recursions of $R_{\mathrm{ud}}^{(p)}$ and $T_{\mathrm{dd}}^{(p)}$ are necessary. Furthermore, if only the reflected diffraction orders are of interest, only recursion of $R_{\mathrm{ud}}^{(p)}$ is necessary.

Note that both exponential functions in (13.139) decay to zero as the layer thickness $\tilde{h}_p$ increases or as the absolute values of the imaginary parts of the eigenvalues increase, thanks to our proper eigenvalue partition. Furthermore, the two exponential functions are not inverted in (13.142). This is the key to the numerical stability of the S-matrix algorithm.

13.6 Concluding Remarks

In this chapter we have presented the basic structure and ingredients of the Fourier modal method. Like most other methods the fields in the homogeneous regions are expanded in Rayleigh expansions. The core idea of the method, as its name says and as Subsections 13.2.1-13.2.3 illustrate, is to solve the modal fields in the grating layer in discrete Fourier space. All other aspects, such as the treatments of slanted grating profile, conical mounting, anisotropic medium, two-dimensional periodicity (crossed grating), are technical details. The modal approach is permitted by the invariance of the grating layer along an out-of-plane direction.

After 50 years of development, the Fourier modal method has become one of the most popular methods, if not the most popular method, for modeling diffraction gratings. However,

it will be wrong to say that it is the best method or it can solve all grating problems. The first statement is wrong because each method has its strength and weakness and without knowing the specifics of a concrete grating problem it is impossible to assess which method is the best for the given problem. The second statement is wrong as we have seen a counterexample in Subsection 13.5.1. In general the Fourier modal method is most suitable to treat gratings with the out-of-plane direction invariance, and its most prominent weakness is its inefficiency or inability to handle metallic gratings without this invariance in TM polarization.

We have assumed that the whole grating surface consists of facets and every facet coincides with a coordinate surface of a suitably chosen skew Cartesian coordinate system. The x^3-invariance is dictated by the modal approach and the top and bottom facets being coincided with two constant x^3 surfaces is required to accommodate the staircase approximation. For the crossed grating problem, the requirement that the other grating facets be parallel to coordinate surfaces of constant x^1 and x^2 is made only to simplify Fourier factorization of the constitutive relations. In real crossed gratings this requirement is often not met and cannot be viewed as a reasonable approximation. In the original work of [13.24] a boundary of arbitrary constant x^3 cross section was approximated by a zigzag boundary, so Fourier factorization can be easily made. This approximation is equivalent to the staircase approximation in the vertical direction, and therefore suffers from the same problem as commented in Subsection 13.5.1. Popov and Nevière [13.34] later found a way to make Fourier factorization without the zigzag approximation. This important contribution to the Fourier factorization theory was first termed fast Fourier factorization, but now the more acceptable term seems to be normal vector field method as proposed by Schuster *et al.* [13.26]. While the x^3-invariance is fundamentally important to the Fourier modal method, there is no reason that the in-plane coordinate system has to be Cartesian. Recently Weiss *et al*. developed the matched-coordinate Fourier modal method [13.7], in which the general x^3-invariant curvilinear coordinate surfaces match the sidewall surface of the crossed gratings. Convergence faster than that of the normal-vector-field method has been achieved. Both the works on the normal-vector-field method and the matched-coordinate method further extend the Fourier modal method and their developments can be fit in the general framework of Section 13.4.

The Fourier modal method relies on the periodicity of the gratings; it is the periodicity that makes discrete Fourier expansion possible. It seems natural to use Fourier basis for analysis of periodic structures; however, Fourier basis has its drawback in handling discontinuous periodic functions because its basis functions are continuous functions. Since mid 1990s and especially in recent years some interesting research works have been done to expand the modal fields in terms of discontinuous basis functions or to use orthogonal polynomial expansions separately for each constant permittivity section of a grating period [13.35-40]. Nonetheless, to date the Fourier basis remains to be the most convenient basis to use.

References

1. M. G. Moharam and T. K. Gaylord, "Rigorous coupled-wave analysis of planar-grating diffraction," J. Opt. Soc. Am. **71**, 811-818 (1981).
2. H. Kogelnik, "Coupled wave theory for thick hologram gratings," Bell Syst. Tech. J. **48**, 2909-2947 (1969).
3. M. G. Moharam, E. B. Grann, D. A. Pommet, and T. K. Gaylord, "Formulation for stable and efficient implementation of the rigorous coupled-wave analysis of binary gratings," J. Opt. Soc. Am. A **12**, 1068-1076 (1995).
4. M. G. Moharam, D. A. Pommet, E. B. Grann, and T. K. Gaylord, "Stable implementation of the rigorous coupled-wave analysis for surface-relief gratings: enhanced transmission matrix approach," J. Opt. Soc. Am. A **12**, 1077-1086 (1995).
5. L. Li, "Mathematical reflections on the Fourier modal method in grating theory," in *Mathematical Modeling in Optical Science*, SIAM (Society for Industrial and Applied Mathematics) Frontiers in Applied Mathematics (SIAM, Philadelphia, 2001), Eds. G. Bao, L. Cowsar, and W. Masters, pp. 111-139.
6. G. Granet, "Reformulation of the lamellar grating problem through the concept of adaptive spatial resolution," J. Opt. Soc. Am. A **16**, 2510-2516 (1999).
7. T. Weiss, G. Granet, N. A. Gippius, S. G. Tikhodeev, and H. Giessen, "Matched coordinates and adaptive spatial resolution in the Fourier modal method," Opt. Express **17**, 8051-8061 (2009).
8. L. Li, "Use of Fourier series in the analysis of discontinuous periodic structures," J. Opt. Soc. Am. A **13**, 1870-1876 (1996).
9. L. Li, "Justification of matrix truncation in the modal methods of diffraction gratings," J. Opt. A: Pure Appl. Opt. **1**, 531-536 (1999).
10. Ph. Lalanne and G. M. Morris, "Highly improved convergence of the coupled-wave method for TM polarization," J. Opt. Soc. Am. A **13**, 779-784 (1996).
11. G. Granet and B. Guizal, "Efficient implementation of the coupled-wave method for metallic lamellar gratings in TM polarization," J. Opt. Soc. Am. A **13**, 1019-1023 (1996).
12. L. Li, "Note on the S-matrix propagation algorithm," J. Opt. Soc. Am. A **20**, 655-660 (2003).
13. L. Li, "Formulation and comparison of two recursive matrix algorithms for modeling layered diffraction gratings," J. Opt. Soc. Am. A **13**, 1024-1035 (1996).
14. E. L. Tan, "Note on formulation of the enhanced scattering- (transmittance-) matrix approach," J. Opt. Soc. Am. A **19**, 1157-1161 (2002).
15. M. G. Moharam and T. K. Gaylord, "Three-dimensional vector coupled-wave analysis of planar grating diffraction," J. Opt. Soc. Am. 7**3**, 1105-1112 (1983).
16. B. Chernov, N. Nevière, and E. Popov, "Fast Fourier factorization method applied to modal method analysis of slanted lamellar diffraction gratings in conical mountings," Opt. Commun. **194**, 289-297 (2001).
17. K. Rokushima and J. Yamakita, "Analysis of anisotropic dielectric gratings," J. Opt. Soc. Am. **73**, 901-908 (1983).

18. E. N. Glytsis and T. K. Gaylord, "Rigorous three-dimensional coupled-wave diffraction analysis of single and cascaded anisotropic gratings," J. Opt. Soc. Am. A **4**, 2061-2080 (1987).

19. S. Mori, K. Mukai, and J. Yamakita, "Analysis of dielectric lamellar gratings coated with anisotropic layers," J. Opt. Soc. Am. A **7**, 1661-1665 (1990).

20. L. Li, "Reformulation of the Fourier modal method for surface-relief gratings made with anisotropic materials," J. Mod. Opt. **45**, 1313-1334 (1998).

21. L. Li, "Oblique-coordinate-system-based Chandezon method for modeling one-dimensionally periodic, multilayer, inhomogeneous, anisotropic gratings," J. Opt. Soc. Am. A, **16**, 2521-2531 (1999).

22. R. Bräuer and O. Bryngdahl, "Electromagnetic diffraction analysis of two-dimensional gratings," Opt. Commun. **100**, 1-5 (1993).

23. E. Noponen and J. Turunen, "Eigenmode method for electromagnetic synthesis of diffractive elements with three-dimensional profiles," J. Opt. Soc. Am. A **11**, 2494-(1994).

24. L. Li, "New formulation of the Fourier modal method for crossed surface-relief gratings," J. Opt. Soc. Am. A **14**, 2758-2767 (1997).

25. L. Li, "Fourier modal method for crossed anisotropic gratings with arbitrary permittivity and permeability tensors," J. Opt. A: Pure Appl. Opt. **5**, 345-355 (2003).

26. T. Schuster, J. Ruoff, N. Kerwien, S. Rafler, and W. Osten, "Normal vector method for convergence improvement using the RCWA for crossed gratings," J. Opt. Soc. Am. A **24**, 2880-2890 (2007).

27. R. Antos, "Fourier factorization with complex polarization bases in modeling optics of discontinuous bi-periodic structures," Opt. Express **17**, 7269-7274 (2009).

28. M. Onishi, K. Crabtree, and R. A. Chipman, "Formulation of rigorous coupled-wave theory for gratings in bianisotropic media," J. Opt. Soc. Am. A, **28**, 1758-(2011).

29. J. van Bladel, *Singular Electromagnetic Fields and Sources* (Clarendon, Oxford, 1991).

30. E. Popov, M. M. Nevière, B. Gralak, and G. Tayeb, "Staircase approximation validity for arbitrary-shaped gratings," J. Opt. Soc. Am. A **19**, 33-42 (2002).

31. L. Li and G. Granet, "Field singularities at lossless metal dielectric right-angle edges and their ramifications to the numerical modeling of gratings," J. Opt. Soc. Am. A **28**, 738-746 (2011).

32. L. Li, "Field singularities at lossless metal dielectric arbitrary-angle edges and their ramifications to the numerical modeling of gratings," J. Opt. Soc. Am. A **29**, 593-604 (2012).

33. L. Li, "Hypersingularity, electromagnetic edge condition, and an analytic hyperbolic wedge model," J. Opt. Soc. Am. A **31** (accepted for publication, Feb. 2014).

34. E. Popov and M. Nevière, "Maxwell equations in Fourier space: fast-converging formulation for diffraction by arbitrary shaped, periodic, anisotropic media," J. Opt. Soc. Am. A **18**, 2886-2894 (2001).

35. R. H. Morf, "Exponentially convergent and numerically efficient solution of Maxwell's equations for lamellar gratings," J. Opt. Soc. Am. A **12**, 1043-1056 (1995).

36. P. Lalanne and J.-P. Hugonin, "Numerical performance of finite-difference modal methods for the electromagnetic analysis of one-dimensional lamellar gratings," J. Opt. Soc. Am. A **17**, 1033-1042 (2000).

37. P. Bouchon, F. Pardo, R. Haïdar, and J.-L. Pelouard, "Fast modal method for subwavelength gratings based on B-spline formulation," J. Opt. Soc. Am. A **27**, 696-702 (2010).

38. G. Granet, L. B. Andriamanampisoa, K. Raniriharinosy, A. M. Armeanu, and K. Edee, "Modal analysis of lamellar gratings using the moment method with subsectional basis and adaptive spatial resolution," J. Opt. Soc. Am. A **27**, 1303-1310 (2010).

39. D. Song, L. Yuan, and Y. Y. Lu, "Fourier-matching pseudospectral modal method for diffraction gratings," J. Opt. Soc. Am. A **28**, 613-620 (2011).

40. K. Edee, "Modal method based on subsectional Gegenbauer polynomial expansion for lamellar gratings," J. Opt. Soc. Am. A **28**, 2006-2013 (2011).